Hamiltonian formulation of nonlinear spin-wave dynamics: Theory and applications

Pavol Krivosik[1,2,*] and Carl E. Patton[1]

[1]*Department of Physics, Colorado State University, Fort Collins, Colorado 80523, USA*
[2]*Slovak University of Technology, Bratislava, Slovak Republic*
(Received 8 July 2010; published 23 November 2010)

A systematic step-by-step development of nonlinear spin-wave theory within the framework of a Hamiltonian formalism is given. The expansion coefficients in the spin-wave Hamiltonian up to the fourth order in the canonical spin-wave amplitudes for a uniformly magnetized ellipsoidal sample are given in general form. This is done for a general orientation of the external field and for a general wave vector. Applications are given for (A) the second-order Suhl spin-wave instability coupling coefficients, (B) the spin-wave wave-vector-dependent nonlinear frequency shift for an in-plane magnetized thin film, and (C) the uniform magnetization mode (ferromagnetic resonance) nonlinear frequency shift for an obliquely magnetized thin film. The analytical results for (C) are compared with results obtained from a time forward numerical analysis of the torque equation of motion and show a near-perfect match.

I. INTRODUCTION

Since the early experiments on ferromagnetic resonance (FMR) at high microwave power levels,[1–3] there have been significant advances in the understanding of large angle magnetization dynamics in ferromagnetic and ferrimagnetic systems. The experimental manifestations of a nonlinear magnetization response are quite varied. They include parametric instability processes,[4,5] auto-oscillations and chaos,[6–8] solitons,[9,10] soliton fractals,[11] and spin momentum transfer (SMT),[12,13] to name a few. These phenomena are realized in a wide range of magnetic materials that range from bulk ferrites to metallic thin film nanostructures.

Most of the early work was focused on parametric instability processes in bulk single-crystal yttrium iron garnet (YIG) materials with extremely low microwave loss.[14,15] Over the past four decades, this work has been extended to polycrystalline[16,17] and thin-film[18,19] ferrites as well as permalloy thin films and microstrips.[20–23] As one specific example, the recent work on high microwave power FMR in permalloy films[24–26] confirmed that the parametric instability processes can take place at relatively small magnetization precession angles, typically below 10° or so, even in relatively high loss ferromagnetic metal. The specific work related to chaos, solitons, and fractals has focused mainly in bulk and thin film single-crystal YIG. The most recent activity in this area is connected to SMT processes, discovered theoretically by Berger and Slonczewski,[27,28] and supported by many subsequent experimental and theoretical advances of both basic and practical interest.[29–33]

From a theoretical point of view, most if not all of above processes can be modeled in terms of the well-developed formalism of elementary magnetic excitations, often termed spin waves or magnons. A theoretical analysis of parametric spin-wave instability (SWI) processes under transverse pumping was given first by Suhl,[34] shortly followed by a theory of parallel pumping SWI processes by Schlömann, Green, and Milano.[35] The general formulation of SWI theory for ferromagnetic insulators with generalized anisotropy and arbitrary pumping field orientation, first done by Patton,[36]

was recently expanded by Nazarov *et al.*[37] The formalism used in most of these works was based on an approach in which the spin-wave dynamic response equations are derived directly from the torque equation of motion for the magnetization $\mathbf{M}(\mathbf{r},t)$ (Ref. 38)

$$\frac{d\mathbf{M}(\mathbf{r},t)}{dt} = -|\gamma|\mathbf{M}(\mathbf{r},t) \times \mathbf{H}_{\text{eff}}(\mathbf{r},t). \quad (1)$$

Here, $\mathbf{r}$ is a general spatial vector, t is the time, γ is the electron gyromagnetic ratio, and $\mathbf{H}_{\text{eff}}(\mathbf{r},t)$ is a net effective field that includes both external and internal field components. Note that the gyromagnetic ratio γ is negative for electrons.

The advantage of the equation-of-motion (EQM) approach is in its intuitive simplicity based directly on the torque equation of motion given above and whatever effective fields may be defined for the problem at hand. The disadvantage of the EQM approach is that any extension of the analysis to new types of interactions or higher order terms in the spin-wave amplitudes is tedious and difficult. The problem lies in the fact that the initial formulation of the dynamics is in terms of the $\mathbf{M}(\mathbf{r},t) \times \mathbf{H}_{\text{eff}}(\mathbf{r},t)$ cross product. In order to solve any specific problem, one must first work out all the terms and then, only at the end, reduce the solution to tractable form.

A more suitable approach for general nonlinear problems in spin-wave dynamics is to transform the torque equation of motion into a scalar Hamiltonian form in terms of canonical variables at the very beginning of the analysis. This done, the problem reduces to (1) a straightforward algebraic extraction of higher order product terms in the Hamiltonian, as needed, and (2) the use of Hamilton's equations to develop the dynamic response. The tedious step here is step (1) but this is mainly a matter of algebra.

Such an approach was, in fact, set out by Schlömann in 1959.[39,40] He established a simple transformation from the dynamic magnetization components of $\mathbf{M}(\mathbf{r},t)$ to conjugate scalar dimensionless canonical variables $a(\mathbf{r},t)$ and $a^*(\mathbf{r},t)$. These same variables transform the basic torque equation of

motion given by Eq. (1) into canonical form. This procedure yields equations of motion for the $a(\mathbf{r},t)$ and $a^*(\mathbf{r},t)$, couched solely in terms of the Hamiltonian of the system in accord with the classical Hamiltonian formalism. This formalism comprises a well-established theoretical approach for weakly nonlinear dissipative systems[41,42] that is widely used for the theoretical analysis of nonlinear wave dynamics in fluid dynamics and atmospheric science,[43–45] plasma physics,[46,47] and, most recently, Bose-Einstein condensates,[48] among others.

Following the seminal work by Schlömann, the Hamiltonian approach has found extensive use for nonlinear problems in spin-wave dynamics. Zakharov, L'vov, and Starobinets (ZLS), for example, extended the Schlömann formalism to the general nonlinear spin-wave problem. These authors made major progress on problems related to spin-wave instability,[49] spin-wave turbulence,[50] inhomogeneity effects,[51] and the statistical behavior of spin-wave systems.[52] Through several books[41,53] and extensive publications, mainly in the Russian literature, the somewhat formal ZLS approach has become, in effect, the *modus operandi* for nonlinear spin-wave theory. Most recently, the Hamiltonian approach has been applied to large-angle spin-wave and magnetization switching dynamics in thin films,[54,55] and to problems in spin momentum transfer.[32,56]

The purpose of this work is to take advantage of the formal simplicity of the Hamiltonian approach outlined above and develop systematic practical working equations that can be applied to a variety of general problems in nonlinear spin-wave dynamics. The approach used in this paper is based on an effective spin-wave tensor formulation, similar to that used by Nazarov *et al.*[37] Note that a similar approach based on Hamiltonian equations of motion and dynamical interaction matrix was proposed recently by Grimsditch *et al.*[57] The focus of Ref. 57, however, was on normal modes and the linear response only. The results in this work, on other hand, are given in general form, for an arbitrary spatially varying and time dependent field in an ellipsoidal sample with uniaxial anisotropy. The final generalized Hamiltonian is given in terms of the normal-mode classical spin-wave amplitudes out to fourth order. In order to obtain tractable equations, however, two simplifying assumptions are invoked. First, the magnetic energy is written as a quadratic functional of the magnetization components. This specific form excludes cubic magnetocrystalline anisotropy, for example, which is a quartic functional of the magnetization components. Second, it is assumed that the normal modes of the sample can be represented as a spatial Fourier plane-wave expansion, e.g., in the form $e^{i\mathbf{k}\cdot\mathbf{r}}$, where $\mathbf{k}$ denotes a general wave vector.

Section II provides a brief outline of the Hamiltonian formalism based on the approach of Schlömann. Section III introduces a formal magnetic sample Hamiltonian function and establishes the basic nomenclature for the detailed term-by-term development to follow. Sections IV and V develop the Hamiltonian expansion coefficients up to fourth order terms in the Fourier spin-wave amplitudes. Up to this point, the theory is maintained in general form. "General form" means that the expansion coefficients are given for arbitrary combinations of wave vectors.

Section VI develops specialized working equations for four-wave processes that are of special interest for spin-wave soliton dynamics, large-angle magnetic switching, and non-linear ferromagnetic resonance under conditions where three-wave processes are prohibited from the point of view of energy and momentum conservation. In the context of this purely classical theory, such prohibited processes may be termed as "nonresonant." The main point is that, even when three-wave processes are nonresonant, it is important to perform a proper transformation to fold in the three-wave Hamiltonian coefficients into the problem in order to obtain a correct result. Section VI presents a short review of this transformation as first developed by Zakharov[58] but cast into practical notation consistent with the development in Secs. I–V.

Section VII presents specific examples of the theory applied to current problems. Section VII A addresses a classical problem of the Suhl second-order spin-wave instability coupling coefficient for ferromagnetic resonance saturation in a uniformly magnetized ellipsoidal sample. Section VII B provides results for the wave-vector-dependent nonlinear spin-wave frequency shift for an in-plane (IP) magnetized thin film. Section VII C examines the nonlinear frequency shift for the uniform FMR mode in thin films. Generally, past developments of the theory for these specific cases do not appear to have taken the Zakharov transformation into proper account in a self-consistent way. Section VIII gives a brief summary. Gaussian cgs units are used throughout the paper.

II. OVERVIEW OF THE HAMILTONIAN FORMALISM

This section provides a brief overview of the basic classical Hamiltonian approach as applied to spin waves in ferromagnetic systems. A comprehensive statement of the method is given by Schlömann (unpublished) in the first actual formulation of the problem cast in this way.[39] A more formal statement of the method is given in Ref. 41. A practical version of the linearized theory and a number of specific applications are given in Ref. 59.

The central point of the classical Hamiltonian approach to spin-wave dynamics lies in the transformation of the classical torque equation for the magnetization vector $\mathbf{M}(\mathbf{r},t)$, as specified in Eq. (1), into a pair of Hamiltonian equations for complex conjugated scalar canonical variables, denoted here as $a(\mathbf{r},t)$ and $a^*(\mathbf{r},t)$. These canonical variables represent temporal and spatial deviations of the magnetization vector from the reference axis that is, in most cases, associated with magnetization static equilibrium. These deviations are generally cast in the form of spin waves. The effective field $\mathbf{H}_{\text{eff}}$ in Eq. (1) is obtained from the Hamiltonian function $\mathcal{H}$ for the sample magnetic energy according to

$$\mathbf{H}_{\text{eff}} = -\frac{1}{V}\frac{\delta\mathcal{H}}{\delta\mathbf{M}}, \qquad (2)$$

where δ denotes a variational derivative and V is the sample volume. The variational derivative form is needed because $\mathcal{H}$ is, in general, a functional of $\mathbf{M}(\mathbf{r},t)$.[59] Note that the both

Eqs. (1) and (2) apply under the assumption that the magnitude of the magnetization vector is constant. This assumption is applicable, strictly speaking, only at low temperature. Based on these working equations, one can develop the general equations of motion for the spin-wave amplitudes in a consistent way.

One starts with a general $\mathbf{M}(\mathbf{r},t)$ and Eqs. (1) and (2). After a series of canonical transformations, one can obtain working equations for $a(\mathbf{r},t)$ and $a^*(\mathbf{r},t)$ in the standard Hamiltonian form. It also proves convenient to cast the conventional $\mathcal{H}$, with units of energy, in terms of a new Hamiltonian function $\mathcal{U}$ with units of frequency. The conversion used here is given by

$$\mathcal{U} = \frac{|\gamma|\mathcal{H}}{M_s V}, \tag{3}$$

where M_s is the saturation magnetization of the material of interest. Note that both $\mathcal{H}$ and $\mathcal{U}$ are real.

As noted above, a suitable canonical transformation that connects the Cartesian magnetization components $M_{x,y,z}(\mathbf{r},t)$ and the canonical variables $a(\mathbf{r},t)$ and $a^*(\mathbf{r},t)$ was first established by Schlömann in the late 1950s.[39,40] Schlömann makes this connection in terms of the magnetization vector direction cosines $\alpha_{x,y,z}(\mathbf{r},t) = M_{x,y,z}(\mathbf{r},t)/M_s$. If one defines a scalar variable $\alpha_\perp(\mathbf{r},t) = i\alpha_x(\mathbf{r},t) + \alpha_y(\mathbf{r},t)$, the $a(\mathbf{r},t)$ and $a^*(\mathbf{r},t)$ are connected to the direction cosines, and hence to $M_{x,y,z}(\mathbf{r},t)$, through

$$\alpha_\perp(\mathbf{r},t) = a(\mathbf{r},t)\sqrt{2 - a(\mathbf{r},t)a^*(\mathbf{r},t)} \tag{4}$$

and

$$\alpha_z(\mathbf{r},t) = 1 - a(\mathbf{r},t)a^*(\mathbf{r},t). \tag{5}$$

The use of a single $\alpha_\perp$ rather than the $\alpha_{x,y}$ separately also leads to a more compact form when the actual Hamiltonian is developed in terms of canonical variables.

Based on this initial transformation, the torque equation of motion in Eq. (1) converts to coupled equations of motion for the $a(\mathbf{r},t)$ and $a^*(\mathbf{r},t)$ in standard Hamiltonian form

$$i\frac{da(\mathbf{r},t)}{dt} = \frac{\delta\mathcal{U}}{\delta a^*(\mathbf{r},t)} \qquad -i\frac{da^*(\mathbf{r},t)}{dt} = \frac{\delta\mathcal{U}}{\delta a(\mathbf{r},t)}. \tag{6}$$

The reader should note the conversion to circular variables through the use of $i\alpha_x + \alpha_y$ rather than the usual $\alpha_x + i\alpha_y$ form. The $i\alpha_x + \alpha_y$ convention chosen here is deliberate. This convention choice is sign-wise consistent with the carryover from $a(\mathbf{r},t)$ and $a^*(\mathbf{r},t)$ to the corresponding quantum annihilation and creation operators $\hat{a}$ and $\hat{a}^\dagger$.

While Ref. 39 was the first statement of the above conversion from the classical torque equation of motion to canonical variables, a quantum-mechanical version of this same transformation for spin waves was first given in the seminal paper of Holstein and Primakoff[60] almost two decades before. The focus of Ref. 60, however, was on the linear theory only. The variables $\alpha_\perp$, $\alpha_\perp^*$, and α_z are classical analogs to the spin operators $\hat{S}^+$, $\hat{S}^-$, and $\hat{S}^z$ in the Holstein-Primakoff (HP) theory. Note that the condition $|\alpha_\perp|^2 + \alpha_z^2 = 1$ is satisfied as a consequence of the conservation of the magnetization magnitude.

In order to cast the problem explicitly in terms of the conventional classical spin waves, the spatial dependences of $a(\mathbf{r},t)$ and $a^*(\mathbf{r},t)$ are expanded as plane-wave Fourier series according to

$$a(\mathbf{r},t) = \sum_\mathbf{k} a_\mathbf{k}(t)e^{i\mathbf{k}\cdot\mathbf{r}} \tag{7}$$

along with the corresponding complex conjugate expression for $a^*(\mathbf{r},t)$. Other basis systems for this expansion are possible, of course, but this spatial plane wave form is convenient to make contact with the properties of traditional spin waves with a general wave vector $\mathbf{k}$ and, in due course, some eigenfrequency $\omega_\mathbf{k}$. Each $a_\mathbf{k}$ and $a_\mathbf{k}^*$ expansion coefficient represents the complex amplitude of a plane spin wave with a propagation direction defined by $\mathbf{k}$. The $\mathbf{k}=0$ mode corresponds to the uniform magnetization mode. Since the Fourier transform is canonical, the equations of motion for the $a_\mathbf{k}$ and $a_\mathbf{k}^*$ retain the same Hamiltonian form as in Eq. (6), namely,

$$i\frac{da_\mathbf{k}(t)}{dt} = \frac{\partial\mathcal{U}}{\partial a_\mathbf{k}^*(t)} \qquad -i\frac{da_\mathbf{k}^*(t)}{dt} = \frac{\partial\mathcal{U}}{\partial a_\mathbf{k}(t)}. \tag{8}$$

The variational derivatives on the right hand side of the expressions in Eq. (6) now appear as partial derivatives in Eq. (8). This replacement follows from the nature of the expansion of the $a(\mathbf{r},t)$ and $a^*(\mathbf{r},t)$ in terms of orthogonal plane waves. It is this expansion that gives a final Hamiltonian function as a polynomial expansion in the $a_\mathbf{k}(t)$ and $a_\mathbf{k}^*(t)$.

Finally, one expands the Hamiltonian function $\mathcal{U}$ in Eq. (8) as an explicit polynomial function in the $a_\mathbf{k}$ and $a_\mathbf{k}^*$ variables. It proves useful to write this expansion in a formal way as $\mathcal{U} = \mathcal{U}^{(0)} + \mathcal{U}^{(1)} + \mathcal{U}^{(2)} + \cdots$ where the superscripts indicate the degree in powers of the different $a_\mathbf{k}$ and $a_\mathbf{k}^*$ products. For example, $\mathcal{U}^{(2)}$ will contain terms proportional to $a_\mathbf{k}a_{\mathbf{k}'}$, $a_\mathbf{k}a_{\mathbf{k}'}^*$, and $a_\mathbf{k}^*a_{\mathbf{k}'}^*$. In case of weakly nonlinear system, this expansion can be limited to selected low order terms, depending on the specific problem of interest. For most problems in spin-wave dynamics, an expansion up to fourth order is usually adequate.

The focus of this paper is on the explicit calculation of the Hamiltonian expansion coefficients up to fourth order. Even though the mechanics of such calculations are reasonably straightforward, the actual implementation can be rather tedious. The main objective of the development in the sections to follows is to provide a step-by-step and reasoned evaluation of the Hamiltonian terms, along with a compilation of final results in a tractable and useful form. As mentioned in Sec. I, many of the previously published expansion coefficients have been generally developed for specific cases and the focus of the papers was generally not on the theory itself. For these reasons, many of these previous statements of the theory have been fragmented, at best. The aim here is to present a cogent, useful, and tractable theory. The present formulation is done in terms of a general 3×3 effective spin-wave tensor $\mathbf{N}_\mathbf{k}$. As defined here, $\mathbf{N}_\mathbf{k}$ takes the same form as the familiar demagnetizing factors for a general ellipsoidal

sample. The theory can be adapted to a wide variety of problems in spin-wave dynamics simply through the appropriate evaluation of the corresponding terms in $\mathbf{N_k}$.

III. MAGNETIC HAMILTONIAN FUNCTION

The objective of this section is to cast the Hamiltonian for the thermodynamic magnetic free energy $\mathcal{H}$, in terms of the Fourier component canonical variables $a_{\mathbf{k}}(t)$ and $a_{\mathbf{k}}^*(t)$. This is most easily done in three steps. A roadmap of these steps is given below. The section closes with further elaboration on some critical details.

A. Roadmap

For the purposes of this analysis, one starts with a generic expression for $\mathcal{H}$ given by

$$\mathcal{H} = -\int \mathbf{M}^T(\mathbf{r},t) \cdot \mathbf{H}_e(\mathbf{r},t) d^3r$$
$$-\frac{1}{2}\int \mathbf{M}^T(\mathbf{r},t) \cdot \mathbf{H}_M(\mathbf{r},t) d^3r - \cdots . \quad (9)$$

The first term represents the Zeeman energy. This term derives from the interaction of the magnetization with an *external* magnetic field $\mathbf{H}_e(\mathbf{r},t) = [H_x(\mathbf{r},t),\ H_y(\mathbf{r},t),\ H_z(\mathbf{r},t)]^T$. For notational simplicity, the "e" subscripts are not shown explicitly in the symbols for the components of $\mathbf{H}_e$. In the algebra to follow, symbols such as $H_{x,y,z}$ and $h_{x,y,z}$ always refer to external fields. The transpose "T" notation for the left side vectors that form scalar or "dot" products is adopted here in anticipation of some of the vector-matrix algebra to follow. In Eq. (9), the right-side vectors are considered as 3×1 column matrices while the left-side-transposed vectors are taken as 1×3 row matrices.

The second term in Eq. (9) represents the interaction energy of the magnetization with an *internal* magnetic self-field $\mathbf{H}_M(\mathbf{r},t)$ that derives from the magnetization itself. For the present purposes, this field is taken as a *linear* functional of the magnetization and written as

$$\mathbf{H}_M(\mathbf{r},t) = -4\pi \int \hat{\mathbf{N}}(\mathbf{r},\mathbf{r}') \cdot \mathbf{M}(\mathbf{r}',t) d^3r' . \quad (10)$$

Here, $\hat{\mathbf{N}}(\mathbf{r},\mathbf{r}')$ is a real 3×3 tensor Green's function operator with components $\hat{N}_{ij}(\mathbf{r},\mathbf{r}')$, i, and $j = x,y,z$. Retardation effects are neglected. The power of this step lies in the fact that all of the magnetic interactions of interest, apart from those due to the external field, are embedded in the $\hat{\mathbf{N}}(\mathbf{r},\mathbf{r}')$ tensor. While adequate for most practical problems of interest, the linear functional form, however, does exclude some effects. Higher order functionals would be needed to deal with cubic magnetocrystalline anisotropy, for example.

In the second step, the Hamiltonian $\mathcal{H}$ is reduced to a simple compact form through three operations, two explicit and one conceptual. The first involves the changeover from $\mathcal{H}$, in energy units, to $\mathcal{U}$, in frequency units, through the $\mathcal{U} = |\gamma| \mathcal{H}/M_s V$ conversion from Sec. II. The second involves a change in variables from $\mathbf{M}(\mathbf{r},t)$ to a direction cosine vector

$\boldsymbol{\alpha}(\mathbf{r},t) = [\alpha_\perp(\mathbf{r},t), \alpha_\perp^*(\mathbf{r},t), \alpha_z(\mathbf{r},t)]^T$, for lack of a better name, according to $\mathbf{M}(\mathbf{r},t) = M_s \mathbf{T} \cdot \boldsymbol{\alpha}(\mathbf{r},t)$. Here, $\mathbf{T}$ is a purely numerical 3×3 matrix given by

$$\mathbf{T} = \frac{1}{2}\begin{pmatrix} -i & i & 0 \\ 1 & 1 & 0 \\ 0 & 0 & 2 \end{pmatrix}. \quad (11)$$

The $\boldsymbol{\alpha}(\mathbf{r},t)$ vector is connected directly to the $a(\mathbf{r},t)$ and $a^*(\mathbf{r},t)$ canonical variables through the Schlömann transformation according to

$$\boldsymbol{\alpha}(\mathbf{r},t) = \begin{bmatrix} \alpha_\perp(\mathbf{r},t) \\ \alpha_\perp^*(\mathbf{r},t) \\ \alpha_z(\mathbf{r},t) \end{bmatrix} = \begin{bmatrix} a(\mathbf{r},t)\sqrt{2 - a(\mathbf{r},t)a^*(\mathbf{r},t)} \\ a^*(\mathbf{r},t)\sqrt{2 - a(\mathbf{r},t)a^*(\mathbf{r},t)} \\ 1 - a(\mathbf{r},t)a^*(\mathbf{r},t) \end{bmatrix}. \quad (12)$$

The conceptual third step involves the use of the above $\boldsymbol{\alpha}(\mathbf{r},t)$ to $a(\mathbf{r},t)$ and $a^*(\mathbf{r},t)$ connections to obtain a $\mathcal{U}$ expression that can be used in the canonical equations of motion embodied in Eq. (6). The caveat, however, is that the nonlinear integrodifferential form of $\mathcal{U}$ generally makes any subsequent analysis unfeasible.

Rather than develop explicit equations form for $\mathcal{U}$ in terms of the $a(\mathbf{r},t)$ and $a^*(\mathbf{r},t)$, the move to canonical form is deferred to step three. Here, a Fourier expansion of $\boldsymbol{\alpha}(\mathbf{r},t)$ is used to develop connections with the Fourier components of the $a(\mathbf{r},t)$ and $a^*(\mathbf{r},t)$, namely, the spin-wave amplitudes $a_{\mathbf{k}}(t)$ and $a_{\mathbf{k}}^*(t)$ as introduced in Sec. II. After expansion of the square-root terms in Eq. (12), with all Fourier transforms folded in, one realizes, at least in concept, a general expression for $\mathcal{U}$ in a practical, polynomial form in terms of the $a_{\mathbf{k}}$ and $a_{\mathbf{k}}^*$. As already noted, the coefficients of the various terms in this expansion, when worked out in explicit form, allow one to solve a wide variety of problems in nonlinear spin-wave dynamics. The process for these operations is given below. The explicit results of the expansions are developed in Sec. IV.

B. Treatment of the external and self fields

Turn back now to the first step in this development, the treatment of the external and self-field terms in the Hamiltonian as broken out in Eq. (9). In order to cast the Hamiltonian formulation into the most general form possible, the external field $\mathbf{H}_e(\mathbf{r},t)$ is retained in a space-time form. That is, the applied field is taken to vary over the sample in a general way be time dependent as well. In the spirit of the spin-wave expansion approach used in the overall development, it is convenient to expand $\mathbf{H}_e(\mathbf{r},t)$ in a similar way. This is done through an expansion in spatial plane waves according to $H_i(\mathbf{r},t) = \Sigma_{\mathbf{k}} H_{i,\mathbf{k}}(t) e^{i\mathbf{k}\cdot\mathbf{r}}$, $i = x,y,z$. This is given in component form. The development to follow will be given explicitly in terms of the $H_{x,\mathbf{k}}(t)$, $H_{y,\mathbf{k}}(t)$, and $H_{z,\mathbf{k}}(t)$. This form folds in an external field in general form and allows for full flexibility for general problems with time varying or spatially inhomogeneous fields. In the usual FMR problem, for example, one would have a homogeneous z-directed static field and a uniform but time-dependent transverse field according to $\mathbf{H}_e(\mathbf{r},t) = [h_{x,0}(t), h_{y,0}(t), H_{z,0}^s]^T$.

The self-field $\mathbf{H_M}(\mathbf{r},t)$, as defined in Eq. (10), can include Maxwellian dipole fields, non-Maxwellian macroscopic exchange fields, and non-Maxwellian effective fields associated with uniaxial anisotropy, for example. Explicit expressions for the corresponding $\hat{\mathbf{N}}(\mathbf{r},\mathbf{r}')$ Green's functions are given in many textbooks. The dipole-dipole interaction energy in the magnetostatic approximation, for example, can be expressed through a Green's function of the form[61]

$$\hat{\mathbf{N}}_{\text{dip}}(\mathbf{r},\mathbf{r}') = \frac{1}{4\pi} \nabla \left(\nabla' \frac{1}{|\mathbf{r}-\mathbf{r}'|} \right). \qquad (13)$$

An isotropic exchange interaction in the macroscopic approximation can be expresses through an $\hat{\mathbf{N}}$ of the form

$$\hat{\mathbf{N}}_{\text{ex}}(\mathbf{r},\mathbf{r}') = -\alpha_{\text{ex}}\delta(\mathbf{r}-\mathbf{r}')\mathbf{I}\,\nabla\cdot\nabla'. \qquad (14)$$

Here, $\alpha_{\text{ex}}=2A/4\pi M_s^2$ is an exchange parameter with units of square centimeters, where A is the exchange energy density, and $\mathbf{I}$ is an identity matrix. For a uniaxial anisotropy one can write $\hat{\mathbf{N}}$ as

$$\hat{\mathbf{N}}_{\text{uniax}}(\mathbf{r},\mathbf{r}') = -\frac{H_u}{4\pi M_s}\delta(\mathbf{r}-\mathbf{r}')\mathbf{e}\otimes\mathbf{e}. \qquad (15)$$

Here, $H_u=2K/M_s$ is an effective uniaxial anisotropy field parameter, K is a uniaxial anisotropy energy density parameter, the unit vector $\mathbf{e}$ defines the direction of the anisotropy axis, and $\otimes$ denotes the dyadic product of two vectors. The Dirac delta function in $\hat{\mathbf{N}}_{\text{ex}}$ and $\hat{\mathbf{N}}_{\text{uniax}}$ expresses the short-range character of the exchange and anisotropy interactions, as opposed to the long-range nature of the dipole-dipole interactions.

Apart from the specific applications in Sec. VII, the analysis here will retain $\hat{\mathbf{N}}(\mathbf{r},\mathbf{r}')$ in general form. This allows for the ready extension of the theory to any specific problem of interest, subject only to the explicit evaluation of the components of the $\hat{\mathbf{N}}$ tensor, or from a more practical point of view, the components of the Fourier transform tensor $\mathbf{N_k}$ that will be introduced shortly.

C. Conversion to the $a(\mathbf{r},t)$ and $a^*(\mathbf{r},t)$

This step is just a matter of algebra. One first folds the $\mathbf{M}(\mathbf{r},t)=M_s\mathbf{T}\cdot\boldsymbol{\alpha}(\mathbf{r},t)$ connection directly into the Hamiltonian function $\mathcal{U}$. As a result, one obtains the $\mathcal{U}$ as a functional of $\boldsymbol{\alpha}(\mathbf{r},t)$. Through the connection given in Eq. (12), $\mathcal{U}$ is also a functional of $a(\mathbf{r},t)$ and $a^*(\mathbf{r},t)$. For the further development of the working equations in standard form, it is also useful to bring in the complex conjugate of $\boldsymbol{\alpha}(\mathbf{r},t)$ through $\boldsymbol{\alpha}^*(\mathbf{r},t)=\mathbf{S}\cdot\boldsymbol{\alpha}(\mathbf{r},t)$, where $\mathbf{S}$ is defined as

$$\mathbf{S} = \begin{pmatrix} 0 & 1 & 0 \\ 1 & 0 & 0 \\ 0 & 0 & 1 \end{pmatrix}. \qquad (16)$$

Based on the above, the Hamiltonian $\mathcal{U}$ can now be written as

$$\mathcal{U} = -\frac{1}{V}\int [\boldsymbol{\alpha}^{\text{T}}(\mathbf{r},t)]^* \cdot |\gamma|\mathbf{H}(\mathbf{r},t)d^3r$$
$$+\frac{1}{2V}\int\int [\boldsymbol{\alpha}^{\text{T}}(\mathbf{r},t)]^* \cdot [\hat{\boldsymbol{\Gamma}}(\mathbf{r},\mathbf{r}')\cdot\boldsymbol{\alpha}(\mathbf{r}',t)]d^3r'd^3r, \qquad (17)$$

where $\mathbf{H}(\mathbf{r},t)$ is a complex vector and $\hat{\boldsymbol{\Gamma}}(\mathbf{r},\mathbf{r}')$ is a complex tensor operator, both defined below.

The complex field vector $\mathbf{H}(\mathbf{r},t)$ is connected to the real external field $\mathbf{H}_{\text{e}}(\mathbf{r},t)$ according to $\mathbf{H}(\mathbf{r},t)=\mathbf{S}\cdot\mathbf{T}^{\text{T}}\cdot\mathbf{H}_{\text{e}}(\mathbf{r},t)$. It proves convenient to write $\mathbf{H}(\mathbf{r},t)$ in explicitly component form according to

$$\mathbf{H}(\mathbf{r},t) = \begin{bmatrix} \dfrac{1}{\sqrt{2}}H_\perp(\mathbf{r},t) \\ \dfrac{1}{\sqrt{2}}H_\perp^*(\mathbf{r},t) \\ H_z(\mathbf{r},t) \end{bmatrix} \qquad (18)$$

with

$$H_\perp(\mathbf{r},t) = \frac{1}{\sqrt{2}}[iH_x(\mathbf{r},t)+H_y(\mathbf{r},t)]. \qquad (19)$$

The numerical $1/\sqrt{2}$ factors are inserted in Eq. (18) in order to give a more compact form for the working equations to follow.

The $\hat{\boldsymbol{\Gamma}}(\mathbf{r},\mathbf{r}')$ operator in Eq. (17) is a transformed version of the original Green's function $\hat{\mathbf{N}}(\mathbf{r},\mathbf{r}')$ defined through

$$\hat{\boldsymbol{\Gamma}}(\mathbf{r},\mathbf{r}') = \omega_M\mathbf{S}\cdot\mathbf{T}^{\text{T}}\cdot\hat{\mathbf{N}}(\mathbf{r},\mathbf{r}')\cdot\mathbf{T}. \qquad (20)$$

The parameter $\omega_M=|\gamma|4\pi M_s$ is used to cast the magnetization into frequency units. In line with the roadmap, the development of $\hat{\boldsymbol{\Gamma}}(\mathbf{r},\mathbf{r}')$ in explicit form is not attempted here. In the next step, the expression for $\mathcal{U}$ is developed in terms of the Fourier transformed amplitudes $a_{\mathbf{k}}$ and $a_{\mathbf{k}}^*$ and in terms of Fourier transformed components of $\mathbf{H}(\mathbf{r},t)$ and $\hat{\boldsymbol{\Gamma}}(\mathbf{r},\mathbf{r}')$. In the end, the entire Hamiltonian function will reduce to relatively simple form in terms of the Fourier components of spin-wave amplitudes, the general space and time-dependent external field, and the initial Green's function tensor $\hat{\mathbf{N}}(\mathbf{r},\mathbf{r}')$ that defines the sample and material of interest.

D. Conversion to the $a_{\mathbf{k}}(t)$ and $a_{\mathbf{k}}^*(t)$

The goal of this last step in the formal development is to obtain the Hamiltonian $\mathcal{U}$ in terms of the $a_{\mathbf{k}}(t)$ and $a_{\mathbf{k}}^*(t)$ spin-wave amplitudes. In parallel with the conversions to $a(\mathbf{r},t)$ and $a^*(\mathbf{r},t)$ used above, this can be done in a compact way with the use of a vector nomenclature. As a first step, however, one expands the direction cosine vector $\boldsymbol{\alpha}(\mathbf{r},t)$ from Eq. (12) in a Fourier series according to

$$\boldsymbol{\alpha}(\mathbf{r},t) = \sum_{\mathbf{k}} \boldsymbol{\alpha}_{\mathbf{k}}(t)e^{i\mathbf{k}\cdot\mathbf{r}}. \qquad (21)$$

Just as the complex $\boldsymbol{\alpha}(\mathbf{r},t)$ vector in Eq. (12) is connected to the spatiotemporal canonical variables $a(\mathbf{r},t)$ and $a^*(\mathbf{r},t)$, the

$a_{\mathbf{k}}(t)$ are connected to the corresponding Fourier transformed spin-wave amplitudes $a_{\mathbf{k}}(t)$ and $a_{\mathbf{k}}^*(t)$. For the time being, the $\boldsymbol{\alpha}_{\mathbf{k}}(t)$ will be written in a generic form as

$$\boldsymbol{\alpha}_{\mathbf{k}}(t) = \begin{bmatrix} \{\alpha_\perp(\mathbf{r},t)\}_{\mathbf{k}} \\ \{\alpha_\perp^*(\mathbf{r},t)\}_{\mathbf{k}} \\ \{\alpha_z(\mathbf{r},t)\}_{\mathbf{k}} \end{bmatrix}, \tag{22}$$

where $\{\dots\}_{\mathbf{k}}$ stands for the Fourier transform. Shortly, the $\boldsymbol{\alpha}_{\mathbf{k}}(t)$ will be developed explicitly in terms of the $a_{\mathbf{k}}(t)$ and $a_{\mathbf{k}}^*(t)$. This will require, however, the use of a Taylor expansion for the square root expression for $\alpha_\perp(\mathbf{r},t)$ in terms of the $a(\mathbf{r},t)$ and $a^*(\mathbf{r},t)$ followed by Fourier transforms to the $a_{\mathbf{k}}(t)$ and $a_{\mathbf{k}}^*(t)$ indicated in Eq. (7).

Turn now to the Fourier transformed components of $\mathbf{H}(\mathbf{r},t)$ and $\hat{\boldsymbol{\Gamma}}(\mathbf{r},\mathbf{r}')$. For the external field, one has

$$\mathbf{H}(\mathbf{r},t) = \sum_{\mathbf{k}} \mathbf{H}_{\mathbf{k}}(t) e^{i\mathbf{k}\cdot\mathbf{r}} \tag{23}$$

with

$$\mathbf{H}_{\mathbf{k}}(t) = \begin{bmatrix} \dfrac{1}{\sqrt{2}} H_{\perp,\mathbf{k}}(t) \\ \dfrac{1}{\sqrt{2}} H_{\perp,-\mathbf{k}}^*(t) \\ H_{z,\mathbf{k}}(t) \end{bmatrix} \tag{24}$$

and $H_{\perp,\mathbf{k}}(t) = [iH_{x,\mathbf{k}}(t) + H_{y,\mathbf{k}}(t)]/\sqrt{2}$.

A proper transform of $\hat{\boldsymbol{\Gamma}}(\mathbf{r},\mathbf{r}')$ is more involved. As a starting point, it proves useful to go back to the properties of $\hat{\mathbf{N}}(\mathbf{r},\mathbf{r}')$. At this point, the formulation also narrows to the explicit consideration of *homogeneous samples only*. The forms for $\hat{\mathbf{N}}_{\mathrm{ex}}(\mathbf{r},\mathbf{r}')$ and $\hat{\mathbf{N}}_{\mathrm{uniax}}(\mathbf{r},\mathbf{r}')$ in Eqs. (14) and (15), for example, assume that the sample is homogeneous, that is, there is no variation in the materials parameters from point to point in the material. In such a case, the general $\hat{\mathbf{N}}(\mathbf{r},\mathbf{r}')$ tensor operator can depend only on the difference $\mathbf{r} - \mathbf{r}'$.

The analysis here also takes the plane wave functions $e^{i\mathbf{k}\cdot\mathbf{r}}$ to be eigenfunctions of the general $\hat{\mathbf{N}}(\mathbf{r}-\mathbf{r}')$ Green's function, in the sense that a Fourier connection of the form

$$\int \hat{\mathbf{N}}(\mathbf{r}-\mathbf{r}') e^{i\mathbf{k}\cdot\mathbf{r}'} d^3 r' = \begin{pmatrix} N_{xx,\mathbf{k}} & N_{xy,\mathbf{k}} & N_{xz,\mathbf{k}} \\ N_{yx,\mathbf{k}} & N_{yy,\mathbf{k}} & N_{yz,\mathbf{k}} \\ N_{zx,\mathbf{k}} & N_{yx,\mathbf{k}} & N_{zz,\mathbf{k}} \end{pmatrix} e^{i\mathbf{k}\cdot\mathbf{r}} = \mathbf{N}_{\mathbf{k}} e^{i\mathbf{k}\cdot\mathbf{r}} \tag{25}$$

is valid. Loosely speaking, the Fourier transform $\mathbf{N}_{\mathbf{k}}$ tensor can be viewed as the corresponding eigenvalue of $\hat{\mathbf{N}}(\mathbf{r}-\mathbf{r}')$, with elements $N_{ij,\mathbf{k}}$ ($i,j=x,y,z$). It is also assumed that the tensorial Green's function $\hat{\mathbf{N}}(\mathbf{r}-\mathbf{r}')$ is symmetric, i.e., the condition $\hat{\mathbf{N}} = \hat{\mathbf{N}}^{\mathrm{T}}$ is satisfied. This implies that $\mathbf{N}_{\mathbf{k}}$ is also symmetric. Such connections are valid for the core $\hat{\mathbf{N}}_{\mathrm{dip}}$, $\hat{\mathbf{N}}_{\mathrm{ex}}$, and $\hat{\mathbf{N}}_{\mathrm{uniax}}$ Green's function tensor operator functions given in Sec. III B.

In the context of this paper, the $\mathbf{N}_{\mathbf{k}}$ will be termed the *effective spin-wave tensor*. This tensor is taken to contain all

necessary information about the spin-wave self-interactions, subject to the validity of the linear form of the self-field $\mathbf{H}_{\mathbf{M}}(\mathbf{r},t)$ functional in Eq. (10). Equation (10), combined with the Fourier expansion $\mathbf{M}(\mathbf{r},t) = \Sigma_{\mathbf{k}} \mathbf{M}_{\mathbf{k}}(t) e^{i\mathbf{k}\cdot\mathbf{r}}$ and Eq. (25) lead directly to a self-field of the form

$$\mathbf{H}_{\mathbf{M}}(\mathbf{r},t) = -4\pi \sum_{\mathbf{k}} \mathbf{N}_{\mathbf{k}} \cdot \mathbf{M}_{\mathbf{k}}(t) e^{i\mathbf{k}\cdot\mathbf{r}}. \tag{26}$$

Note that $\mathbf{N}_{\mathbf{k}}$ can be defined through Eq. (25) and (26). One form or the other may be easier to implement, depending on the specific problem at hand. These authors find, for example, that the $\mathbf{N}_{\mathbf{k}}$ for dipole-dipole interactions is easier to obtain from Eq. (26). In this case, one first obtains the spatiotemporal dipole field connected to $\mathbf{M}(\mathbf{r},t)$ and takes the Fourier transform. In contrast, the direct transform of $\hat{\mathbf{N}}(\mathbf{r},\mathbf{r}')$ involves nine separate component terms that can make the analysis cumbersome and tedious.

Turn now to the properties of the general $\mathbf{N}_{\mathbf{k}}$ tensor. Since both $\mathbf{M}(\mathbf{r},t)$ and $\mathbf{H}_{\mathbf{M}}(\mathbf{r},t)$ are real, the condition $\mathbf{N}_{-\mathbf{k}} = \mathbf{N}_{\mathbf{k}}^*$ must be satisfied. From the fact that the Hamiltonian function $\mathcal{H}$ is real, one can also show that the $\mathbf{N}_{\mathbf{k}}$ is self-adjoint, that is, $\mathbf{N}_{\mathbf{k}} = (\mathbf{N}_{\mathbf{k}}^{\mathrm{T}})^*$ is valid. These two properties, in combination with the assumption that $\mathbf{N}_{\mathbf{k}}$ is a symmetric tensor, imply that $\mathbf{N}_{\mathbf{k}}$ is real and equal to $\mathbf{N}_{-\mathbf{k}}$. While these properties clearly apply for the self-fields for dipole-dipole and exchange interactions and for uniaxial anisotropy, these authors know of no general proof for these interconnected properties.

The conversion from the physical micromagnetic Green's function tensor $\hat{\mathbf{N}}(\mathbf{r}-\mathbf{r}')$ to an effective spin-wave tensor $\mathbf{N}_{\mathbf{k}}$, as in Eq. (25), is a key element in this formulation of nonlinear magnetization dynamics. As will be made clear shortly, this conversion greatly simplifies the analysis for this formidable problem. In what follows, the $\mathbf{N}_{\mathbf{k}}$ will be kept in a general form. Specialized expressions for the $\mathbf{N}_{\mathbf{k}}$ components will be given in Sec. VII as specific applications are considered.

Based on the above, the Hamiltonian function $\mathcal{U}$ in frequency units can be now written in simple form in terms of the various Fourier elements that have been developed above. The result is a rather tractable $\mathcal{U}$ expression that takes the form

$$\mathcal{U} = -\sum_{\mathbf{k}} [\boldsymbol{\alpha}_{\mathbf{k}}^{\mathrm{T}}(t)]^* |\gamma| \mathbf{H}_{\mathbf{k}}(t) + \frac{1}{2} \sum_{\mathbf{k}} [\boldsymbol{\alpha}_{\mathbf{k}}^{\mathrm{T}}(t)]^* [\boldsymbol{\Gamma}_{\mathbf{k}} \cdot \boldsymbol{\alpha}_{\mathbf{k}}(t)] \tag{27}$$

with $\boldsymbol{\Gamma}_{\mathbf{k}} = \omega_M \mathbf{S} \cdot \mathbf{T}^{\mathrm{T}} \cdot \mathbf{N}_{\mathbf{k}} \cdot \mathbf{T}$. After some straightforward matrix multiplication and collection of terms, one can also obtain $\boldsymbol{\Gamma}_{\mathbf{k}}$ in explicit term-by-term form, according to

$$\boldsymbol{\Gamma}_{\mathbf{k}} = \begin{bmatrix} \dfrac{1}{2} Q_{\mathbf{k}} & \dfrac{1}{2} B_{\mathbf{k}} & \dfrac{1}{\sqrt{2}} D_{\mathbf{k}} \\ \dfrac{1}{2} B_{\mathbf{k}}^* & \dfrac{1}{2} Q_{\mathbf{k}} & \dfrac{1}{\sqrt{2}} D_{\mathbf{k}}^* \\ \dfrac{1}{\sqrt{2}} D_{\mathbf{k}}^* & \dfrac{1}{\sqrt{2}} D_{\mathbf{k}} & \Gamma_{zz,\mathbf{k}} \end{bmatrix} \tag{28}$$

with

$$Q_{\mathbf{k}} = \frac{\omega_M}{2}(N_{xx,\mathbf{k}} + N_{yy,\mathbf{k}}), \tag{29}$$

$$B_{\mathbf{k}} = \frac{\omega_M}{2}(-N_{xx,\mathbf{k}} + N_{yy,\mathbf{k}} + 2iN_{xy,\mathbf{k}}), \tag{30}$$

$$D_{\mathbf{k}} = \frac{\omega_M}{\sqrt{2}}(iN_{xz,\mathbf{k}} + N_{yz,\mathbf{k}}) \tag{31}$$

and

$$\Gamma_{zz,\mathbf{k}} = \omega_M N_{zz,\mathbf{k}}. \tag{32}$$

Since $\mathcal{U}$ is real, the $\Gamma_{\mathbf{k}}$ tensor must be self-adjoint. This condition, in turn, implies that the diagonal $Q_{\mathbf{k}}$ and $\Gamma_{zz,\mathbf{k}}$ components of $\Gamma_{\mathbf{k}}$ must be real as well. This conclusion also follows from the fact that the $N_{\mathbf{k}}$ tensor is real.

Equation (27) gives the system energy directly in terms of a sum over various combinations of the Fourier vector $\boldsymbol{\alpha}_{\mathbf{k}}(t)$ with the known physical parameters of the system $H_{\mathbf{k}}$ and $N_{\mathbf{k}}$. The final step for this section is to carry this forward to obtain the Hamiltonian as an expansion of terms to various orders in the $a_{\mathbf{k}}$ and $a_{\mathbf{k}}^*$ spin-wave amplitude outlined in the introduction. This procedure would be straightforward and algebraically simple, except for the fact that there is no simple direct analytical connection between the $\boldsymbol{\alpha}_{\mathbf{k}}(t)$ and the $a_{\mathbf{k}}(t)$ and $a_{\mathbf{k}}^*(t)$. The problem lies in the appearance of square root terms in the connection between the original direction cosine vector for the magnetization, $\boldsymbol{\alpha}(\mathbf{r},t)$, and the original $a(\mathbf{r},t)$ and $a^*(\mathbf{r},t)$ canonical variables. From Eq. (12), for example, the transverse $\alpha_{\perp}(\mathbf{r},t)$ component has a form $\alpha_{\perp}(\mathbf{r},t) = a(\mathbf{r},t)\sqrt{2 - a(\mathbf{r},t)a^*(\mathbf{r},t)}$. In order to obtain the Fourier component $\{\alpha_{\perp}(\mathbf{r},t)\}_{\mathbf{k}}$ in terms of the $a_{\mathbf{k}}$ and $a_{\mathbf{k}}^*$, one must first expand the square root in $\alpha_{\perp}(\mathbf{r},t)$ and then insert proper Fourier expansion forms for the $a(\mathbf{r},t)$ and $a^*(\mathbf{r},t)$ terms therein.

In order to keep the analysis tractable, the square-root expansion of $\alpha_{\perp}(\mathbf{r},t)$ will be limited to the first two terms, according to

$$\alpha_{\perp}(\mathbf{r},t) \approx \sqrt{2}\, a(\mathbf{r},t)\left[1 - \frac{1}{4} a(\mathbf{r},t)a^*(\mathbf{r},t)\right]. \tag{33}$$

The error in such a two term form is small. The above gives $|\alpha_{\perp}|^2 + \alpha_z^2 = 1 + |a|^6/8$ instead of the exact value of 1. Keep in mind that $|a|$ is on the order of $|\alpha_{\perp}|$. For a simple circularly polarized uniform precession response, one can show that $|a|$ is equal to $\sqrt{1 - \cos\phi}$, where ϕ is the precession angle. This yields an error in the two term expansion on the order of 10%, even for precession angles close to 90°, for example.

The components of the $\boldsymbol{\alpha}_{\mathbf{k}}(t)$ vector in Eq. (22) can now be found from the Fourier transforms of the expanded $\alpha_{\perp}(\mathbf{r},t)$ from Eq. (33), the corresponding complex conjugate, and the $\alpha_z(\mathbf{r},t)$ from Eq. (5). For $\{\alpha_{\perp}(\mathbf{r},t)\}_{\mathbf{k}}$, Fourier transform algebra gives

$$\{\alpha_{\perp}(\mathbf{r},t)\}_{\mathbf{k}} = \frac{1}{V}\int \alpha_{\perp}(\mathbf{r},t)e^{-i\mathbf{k}\cdot\mathbf{r}}d^3r$$
$$\approx \sqrt{2}\left\{ a_{\mathbf{k}}(t) - \frac{1}{4}\sum_{\mathbf{k}_1\mathbf{k}_2\mathbf{k}_3}[a_{\mathbf{k}_1}(t)a_{\mathbf{k}_2}(t)a_{\mathbf{k}_3}^*(t)\right.$$
$$\times\Delta(\mathbf{k}_1 + \mathbf{k}_2 - \mathbf{k}_3 - \mathbf{k})]\Bigg\}$$
$$\equiv \sqrt{2}\left\{ a_{\mathbf{k}}(t) - \frac{1}{4}\sum_{\mathbf{123}}[a_1(t)a_2(t)a_3^*(t)\right.$$
$$\times\Delta(\mathbf{1} + \mathbf{2} - \mathbf{3} - \mathbf{k})]\Bigg\}. \tag{34}$$

Here, Δ is a Kronecker delta function that follows from $\int e^{\pm i\mathbf{k}\cdot\mathbf{r}}d^3r = V\Delta(\mathbf{k})$. The last line of Eq. (34) uses a standard shorthand notation with $\mathbf{k}_1 \equiv \mathbf{1}$, $\mathbf{k}_2 \equiv \mathbf{2}$, ..., and $\Delta(\mathbf{k}_1 - \mathbf{k}_2 - \mathbf{k}) \equiv \Delta(\mathbf{1} - \mathbf{2} - \mathbf{k})$, etc.[41,42] All working equations from this point forward will incorporate this shorthand notation for sum terms with more than one $\mathbf{k}$ index. Fourier transform algebra yields corresponding expressions for $\{\alpha_{\perp}^*(\mathbf{r},t)\}_{\mathbf{k}}$ and $\{\alpha_z(\mathbf{r},t)\}_{\mathbf{k}}$.

$$\{\alpha_{\perp}^*(\mathbf{r},t)\}_{\mathbf{k}} \approx \sqrt{2}\left[a_{-\mathbf{k}}^*(t) - \frac{1}{4}\sum_{\mathbf{123}} a_1^*(t)a_2^*(t)a_3(t)\right.$$
$$\times\Delta(\mathbf{1} + \mathbf{2} - \mathbf{3} + \mathbf{k})\Bigg]. \tag{35}$$

$$\{\alpha_z(\mathbf{r},t)\}_{\mathbf{k}} = \Delta(\mathbf{k}) - \sum_{\mathbf{12}} a_1(t)a_2^*(t)\Delta(\mathbf{1} - \mathbf{2} - \mathbf{k}). \tag{36}$$

Equations (34)–(36) give explicit expressions for the terms in $\boldsymbol{\alpha}_{\mathbf{k}}(t)$ given formally in Eq. (22). These specific functions may now be used in the Hamiltonian of Eq. (27) to obtain $\mathcal{U}(a_{\mathbf{k}}, a_{\mathbf{k}}^*)$. Keep in mind that apart from the $a_{\mathbf{k}}$ and $a_{\mathbf{k}}^*$ factors in $\mathcal{U}$ that derive from Eqs. (34)–(36), all of the components of $\mathcal{U}$ involve only experimental or materials parameters embedded in the $H_{\mathbf{k}}(t)$ Fourier components of the external field and the $N_{\mathbf{k}}$ Fourier components of the effective spin-wave tensor.

IV. HAMILTONIAN EXPANSION COEFFICIENTS

The only remaining task in terms of the formal theory is in the collection of the various order terms in $a_{\mathbf{k}}(t)$ and $a_{\mathbf{k}}^*(t)$ for the Taylor expanded master $\mathcal{U}(a_{\mathbf{k}}, a_{\mathbf{k}}^*)$ Hamiltonian function. Recall the form of this Hamiltonian given in Sec. II, $\mathcal{U} = \mathcal{U}^{(0)} + \mathcal{U}^{(1)} + \mathcal{U}^{(2)} + \cdots$ The subsections below will present the general expressions for the $\mathcal{U}^{(n)}$ out to $n = 4$. The $\mathcal{U}^{(0)}$ term contains no $a_{\mathbf{k}}$ or $a_{\mathbf{k}}^*$ factors and corresponds to the ground-state energy in the absence of any spin-wave excitations. Insofar as $\partial\mathcal{U}^{(0)}/\partial a_{\mathbf{k}}$ and $\partial\mathcal{U}^{(0)}/\partial a_{\mathbf{k}}^*$ are both zero, the zeroth-order term in $\mathcal{U}$ has no effect on the dynamics. The $\mathcal{U}^{(1)}$ term contains single $a_{\mathbf{k}}$ or $a_{\mathbf{k}}^*$ factors. The corresponding $\partial\mathcal{U}^{(1)}/\partial a_{\mathbf{k}}$ and $\partial\mathcal{U}^{(1)}/\partial a_{\mathbf{k}}^*$ operations applied to the Hamiltonian equations of motion from Eq. (8) lead to (1) static equilibrium and (2) the dynamic pumping of the $a_{\mathbf{k}}(t)$ and $a_{\mathbf{k}}^*(t)$ by any

time-dependent external transverse x, y fields that may present in the system. A spatially uniform dynamic pumping signal, in combination with terms from $\mathcal{U}^{(2)}$ at $\mathbf{k}=0$, for example, leads to driven ferromagnetic resonance.

It is the $\mathcal{U}^{(2)}$, $\mathcal{U}^{(3)}$, and $\mathcal{U}^{(4)}$ terms that lead to the effects that are important in linear and nonlinear spin-wave dynamics. The $\mathcal{U}^{(2)}$ term, in itself, leads to the linear spin-wave dispersion. This will become clear in Sec. V when the $\mathcal{U}^{(2)}$ term will be diagonalized by a linear transformation to define the normal spin-wave modes of the linear system.

The $\mathcal{U}^{(3)}$ term leads to so-called three-wave processes. In the quantum picture, this corresponds to a situation in which one magnon splits into two magnons, schematically indicated as $(\mathbf{1}) \rightarrow (\mathbf{2}, \mathbf{3})$, or in which two magnons combine to produce a third magnon, shown as $(\mathbf{1}, \mathbf{2}) \rightarrow (\mathbf{3})$. These interactions must conserve both energy and momentum and are allowed, therefore, only under certain conditions that depend on the sample properties and the magnetic field. Even when such resonant processes are not allowed, however, the $\mathcal{U}^{(3)}$ term in the Hamiltonian can still play a role in higher order processes. This important point will be developed in the applications discussion to follow.

The $\mathcal{U}^{(4)}$ term leads to so-called four-wave processes. The quantum picture here can be illustrated as $(\mathbf{1}) \rightarrow (\mathbf{2}, \mathbf{3}, \mathbf{4})$, $(\mathbf{1}, \mathbf{2}) \rightarrow (\mathbf{3}, \mathbf{4})$, and $(\mathbf{1}, \mathbf{2}, \mathbf{3}) \rightarrow (\mathbf{4})$. The two in and two out case, $(\mathbf{1}, \mathbf{2}) \rightarrow (\mathbf{3}, \mathbf{4})$, is the most important for practical problems because such processes are always allowed, independent of the sample properties or the field. In spin-wave dynamics problems, the term "four-wave processes" usually refers to this subclass of interactions.

The sections to follow will serve to as a guide to the compilation of Hamiltonian coefficients for these various order terms in $\mathcal{U}$ up to $\mathcal{U}^{(4)}$ in the form indicated above and based on the canonical $a_{\mathbf{k}}$ and $a_{\mathbf{k}}^*$ spin-wave amplitudes. Following this compilation, Sec. V will then present a further conversion of all $\mathcal{U}$ terms up to fourth order that make explicit, among other things, the important operating terms for spin-wave soliton dynamics, as well as Suhl first- and second-order spin-wave instability processes.

A. Zeroth-order $\mathcal{U}^{(0)}$—ground-state energy

As noted above, the zeroth-order $\mathcal{U}^{(0)}$ term contains no $a_{\mathbf{k}}$ or $a_{\mathbf{k}}^*$ variables and basically represents a zero-point magnetic energy. As such, this term contributes nothing to the spin-wave dynamics of the system. It is included here, mainly for completeness. From the component equations listed previously, one obtains

$$\mathcal{U}^{(0)} = -|\gamma| H_{z,0}(t) + \frac{1}{2} \Gamma_{zz,0} \qquad (37)$$

or in terms of the original Hamiltonian

$$\mathcal{H}^{(0)} = V\left[-H_{z,0}(t) M_s + \frac{1}{2} 4\pi N_{zz,0} M_s^2 \right]. \qquad (38)$$

Recall that $H_{z,0}(t)$ is the spatially uniform $\mathbf{k}=0$ z component of the external field and $N_{zz,0}$ is an effective static demagnetizing factor in the z direction. The zeroth order energy,

therefore, simply gives the ground state Zeeman plus demagnetizing field energy for a uniformly magnetized sample in a uniform z-directed field.

B. First-order $\mathcal{U}^{(1)}$—transverse fields

After all linear terms in the $a_{\mathbf{k}}$ and $a_{\mathbf{k}}^*$ amplitudes are collected, the first-order term $\mathcal{U}^{(1)}$ in the energy expansion can be written as

$$\mathcal{U}^{(1)} = -\sum_{\mathbf{k}} F_{\mathbf{k}}^*(t) a_{\mathbf{k}}(t) + \text{c.c.} \qquad (39)$$

where c.c. stands for the complex conjugate of the preceding term. The $F_{\mathbf{k}}(t)$ coefficient is given as

$$F_{\mathbf{k}}(t) = |\gamma| H_{\perp, \mathbf{k}}(t) - D_{\mathbf{k}} \Delta(\mathbf{k}). \qquad (40)$$

Here, the $H_{\perp, \mathbf{k}}(t)$ represent the Fourier transform of transverse x and y components of the external magnetic field that follows from Eq. (24). The $D_{\mathbf{k}}$ are given in Eq. (31).

Recall that $\mathcal{U}^{(1)}$ leads to static equilibrium and the linear response to a transverse time-dependent pumping field. For the further elaboration of these considerations, it is useful to break out $H_{\perp, \mathbf{k}}(t)$ into separate static and time-dependent terms according to $H_{\perp, \mathbf{k}}(t) = H_{\perp, \mathbf{k}}^s + h_{\perp, \mathbf{k}}(t)$. From here on, a capital H^s will be use to denote purely static fields and lower case h will denote time dependent fields. Recall also that the $H_\perp$ notation folds in both the x- and y-field components into a single complex scalar field parameter according to $H_\perp = (iH_x + H_y)/\sqrt{2}$.

As an example of the equilibrium problem, consider the special case of a homogeneous transverse field only. In this situation, $\mathcal{U}^{(1)}$ becomes

$$\mathcal{U}^{(1)} = (-|\gamma| H_{\perp,0}^{s*} + D_0^*) a_0(t) - |\gamma| h_{\perp,0}^*(t) a_0(t) + \text{c.c.} \quad (41)$$

This equation, in combination with corresponding terms from $\mathcal{U}^{(2)}$, will lead to a linear equation of motion for $a_0(t)$ that also contains an $(-|\gamma| H_{\perp,0}^s + D_0)$ factor with no $a_0(t)$ multiplier. The corresponding condition

$$-|\gamma| H_{\perp,0}^s + D_0 = 0 \qquad (42)$$

defines static equilibrium. In x-y component form, one has $H_{x,0}^s = 4\pi M_s N_{xz,0}$ and $H_{y,0}^s = 4\pi M_s N_{yz,0}$. These equations correspond to the well-known condition for the static equilibrium in a uniformly magnetized sample. One will also have a time dependent $|\gamma| h_{\perp,0}^*(t)$ driving term in the equation of motion for $a_0(t)$. This term usually corresponds to the microwave pump field in standard ferromagnetic resonance experiments. This term, in combination with additional equation of motion terms from $\mathcal{U}^{(2)}$ with $a_0(t)$ and $a_0^*(t)$ factors, lead to the well-known working equations for the uniform-mode FMR response.

C. Second-order $\mathcal{U}^{(2)}$—linear modes

The general form of the $\mathcal{U}^{(2)}$ term in the Hamiltonian expansion may be obtained as

$$\mathcal{U}^{(2)} = \sum_{12} |\gamma| H_{z,1-2}(t) a_1^*(t) a_2(t) + \sum_{\mathbf{k}} \left[(Q_{\mathbf{k}} - \Gamma_{zz,0}) a_{\mathbf{k}}^*(t) a_{\mathbf{k}}(t) \right.$$
$$\left. + \frac{B_{\mathbf{k}}}{2} a_{\mathbf{k}}^*(t) a_{-\mathbf{k}}^*(t) + \frac{B_{\mathbf{k}}^*}{2} a_{\mathbf{k}}(t) a_{-\mathbf{k}}(t) \right]. \tag{43}$$

Keep in mind that the $\Gamma_{zz,0}$, $Q_{\mathbf{k}}$, and the $B_{\mathbf{k}}$ parameters contain various combinations of terms from the original effective spin-wave tensor $\mathbf{N_k}$ as developed in the previous section. The leading double sum term in the above represents a potential pairwise coupling between all spin waves. The coupling between spin waves with different $\mathbf{k}$ values, however, depends on the spatial nature of $H_z(\mathbf{r},t)$ and the size of a given Fourier component at wave vector $\mathbf{k}_1-\mathbf{k}_2$, for example. The second single sum term involves pairs of spin waves with the same or opposite $\mathbf{k}$ values. The coupling of these terms is possible for a general system, even one with strictly spatially homogeneous fields.

Two special cases can be used to elucidate the physics contained in $\mathcal{U}^{(2)}$. Case I. Consider the situation in which the z component of the external field is spatially homogeneous and time independent, such that $H_{z,\mathbf{k}}(t)$ is equal to some $H_{z,0}^s$ only. In this case, $\mathcal{U}^{(2)}$ takes the familiar form from linear spin-wave theory

$$\mathcal{U}^{(2)} = \sum_{\mathbf{k}} \left[A_{\mathbf{k}} a_{\mathbf{k}}^*(t) a_{\mathbf{k}}(t) + \frac{B_{\mathbf{k}}}{2} a_{\mathbf{k}}^*(t) a_{-\mathbf{k}}^*(t) + \frac{B_{\mathbf{k}}^*}{2} a_{\mathbf{k}}(t) a_{-\mathbf{k}}(t) \right] \tag{44}$$

with

$$A_{\mathbf{k}} = |\gamma| H_{z,0}^s - \Gamma_{zz,0} + Q_{\mathbf{k}} = \omega_H + \frac{\omega_M}{2}(N_{xx,\mathbf{k}} + N_{yy,\mathbf{k}}). \tag{45}$$

In the above the spatially uniform internal static field H_i has been cast into frequency units through the parameter

$$\omega_H = |\gamma| H_i = |\gamma|(H_{z,0}^s - 4\pi M_s N_{zz,0}). \tag{46}$$

Note that the $A_{\mathbf{k}}$ expression in Eq. (45) folds in nonvanishing contributions from the double sum term in Eq. (43) for $\mathbf{k}_1 = \mathbf{k}_2$ as well the obvious contributions from the single sum term. The $A_{\mathbf{k}}$ and $B_{\mathbf{k}}$ coefficients will play an important role in Sec. V for the diagonalization procedure to obtain the normal spin-wave modes and the frequency wave-vector spin-wave dispersion relation for the linear system.

Case II. If the z component of the spatially homogeneous external field contains a dynamic component, taken as $h_z(t)$, one obtains what has been termed "parallel pumping," an important parametric process initially discovered by Schlömann, Green, and Milano.[35] For this process, there will be a $\mathcal{U}^{(2)}$ term that takes the form $\Sigma_{\mathbf{k}} |\gamma| h_{z,0}(t) a_{\mathbf{k}}^*(t) a_{\mathbf{k}}(t)$. For elliptically polarized modes, the application of a parallel pump field $h_z(t)$ above a certain threshold leads to the parametric excitation of spin-wave pairs with wave vectors of $\pm\mathbf{k}$.

D. Third-order $\mathcal{U}^{(3)}$—three-wave processes

From a direct collection of terms, the $\mathcal{U}^{(3)}$ term in the Hamiltonian is obtained as

$$\mathcal{U}^{(3)} = \frac{1}{4} \sum_{123\mathbf{k}} [|\gamma| H_{\perp,\mathbf{k}}^*(t) a_1(t) a_2(t) a_3^*(t) + \text{c.c.}] \Delta(\mathbf{1} + \mathbf{2} - \mathbf{3} - \mathbf{k})$$
$$- \frac{1}{2} \sum_{123} [(D_1^* + D_2^* + D_0^*/2) a_1(t) a_2(t) a_3^*(t) + \text{c.c.}] \Delta(\mathbf{1} + \mathbf{2} - \mathbf{3}). \tag{47}$$

As with $\mathcal{U}^{(2)}$, all parameters are defined explicitly either through the known applied field or, in the case of the $D_{\mathbf{k}}$ terms, through the $\mathbf{N_k}$ tensor. The physics in $\mathcal{U}^{(3)}$ can be seen more easily if one, as before, breaks $H_{\perp,0}(t)$ into static and dynamic components according to $H_{\perp,0}(t)=H_{\perp,0}^s+h_{\perp,0}(t)$ and rewrites Eq. (47) in a different form. With this replacement, one may use the equilibrium condition from Eq. (42), $-|\gamma| H_{\perp,0}^s + D_0 = 0$, to combine and then eliminate the $|\gamma| H_{\perp,0}^s$ and D_0 terms in the sums above and obtain

$$\mathcal{U}^{(3)} = \frac{1}{4} \sum_{123} [|\gamma| h_{\perp,0}^*(t) a_1(t) a_2(t) a_3^*(t) + \text{c.c.}] \Delta(\mathbf{1} + \mathbf{2} - \mathbf{3})$$
$$+ \frac{1}{4} \sum_{\substack{123 \\ \mathbf{k} \neq 0}} [|\gamma| H_{\perp,\mathbf{k}}^*(t) a_1(t) a_2(t) a_3^*(t) + \text{c.c.}]$$
$$\times \Delta(\mathbf{1} + \mathbf{2} - \mathbf{3} - \mathbf{k}) - \frac{1}{2} \sum_{123} [(D_1^* + D_2^*) a_1(t) a_2(t) a_3^*(t)$$
$$+ \text{c.c.}] \Delta(\mathbf{1} + \mathbf{2} - \mathbf{3}). \tag{48}$$

Even though Eq. (48) looks, at first glance, more formidable that Eq. (47), the three sum terms can be interpreted in a more direct way.

The first sum describes a process in which a quantum of the electromagnetic wave from the spatially homogeneous external transverse pump field represented by $h_{\perp,0}$ interacts with a spin-wave excitation a_3 accompanied by destruction of two another spin-wave excitations a_1 and a_2, along with the opposite process signified by the "c.c." The Kronecker delta function serves to conserve wave vector among the three magnons involved in the scattering process. The scattering process described by this sum belongs to the class of *four-wave* processes and enters the analysis of premature saturation of main resonance, for example.[37]

The second sum represents the nonlinear interaction between different spin-wave modes due to the presence of any spatially inhomogeneous external transverse field components, represented by $H_{\perp,\mathbf{k}}$. In most cases this term can be omitted since the usual experimental configuration involve spatially homogeneous external fields.

The third sum gives the pure nonlinear coupling between three spin-wave modes. The special case for no external transverse field is important for later discussion. In this case, only the third term remains and the third-order Hamiltonian reduces to

$$\mathcal{U}^{(3)} \approx -\frac{1}{2} \sum_{\mathbf{123}} [(D_{\mathbf{1}}^* + D_{\mathbf{2}}^*) a_{\mathbf{1}}(t) a_{\mathbf{2}}(t) a_{\mathbf{3}}^*(t) + \text{c.c.}] \Delta(\mathbf{1} + \mathbf{2} - \mathbf{3}).$$

(49)

In most FMR and spin-wave relaxation rate and linewidth analyses, this form of $\mathcal{U}^{(3)}$ is commonly understood as the "three-wave process" term.

E. Fourth-order $\mathcal{U}^{(4)}$—four-wave processes

The fourth-order $\mathcal{U}^{(4)}$ term can be written as

$$\mathcal{U}^{(4)} = \frac{1}{2} \sum_{\mathbf{1234}} \Psi_{\mathbf{12},(-\mathbf{3})(-\mathbf{4})} a_{\mathbf{1}}(t) a_{\mathbf{2}}(t) a_{\mathbf{3}}^*(t) a_{\mathbf{4}}^*(t) \Delta(\mathbf{1} + \mathbf{2} - \mathbf{3} - \mathbf{4})$$

$$+ \frac{1}{3} \sum_{\mathbf{1234}} [\Phi_{\mathbf{123},\mathbf{4}}^* a_{\mathbf{1}}(t) a_{\mathbf{2}}(t) a_{\mathbf{3}}(t) a_{\mathbf{4}}^*(t) + \text{c.c.}]$$

$$\times \Delta(\mathbf{1} + \mathbf{2} + \mathbf{3} - \mathbf{4}) \quad (50)$$

with

$$\Psi_{\mathbf{12},\mathbf{34}} = -\frac{1}{4}(Q_1 + Q_2 + Q_3 + Q_4) + \frac{1}{4}(\Gamma_{zz,\mathbf{1}+\mathbf{3}} + \Gamma_{zz,\mathbf{1}+\mathbf{4}}$$

$$+ \Gamma_{zz,\mathbf{2}+\mathbf{3}} + \Gamma_{zz,\mathbf{2}+\mathbf{4}}) \quad (51)$$

and

$$\Phi_{\mathbf{123},\mathbf{4}} = -\frac{1}{4}(B_1 + B_2 + B_3). \quad (52)$$

While the expansion coefficients for these four-wave sum terms appear formidable, it is important to keep in mind that all terms are defined explicitly through the $\mathbf{N_k}$ tensor. Even though the $\Phi_{\mathbf{123},\mathbf{4}}$ coefficient is shown as a sum of B_1, B_2, and B_3 terms only, one also has an implicit dependence on the $\mathbf{k}_4$ wave-vector index through the $\Delta(\mathbf{1}+\mathbf{2}+\mathbf{3}-\mathbf{4})$ constraint in Eq. (50).

Brief remarks are in order at this point with regard to the indexing scheme used for the $\Psi_{\mathbf{12},\mathbf{34}}$ and $\Phi_{\mathbf{123},\mathbf{4}}$ coefficients in the above. The comma separators relate to rules for interchangeability. In general, of course, one can always interchange or relabel dummy indices with no effect on the overall equation of interest. Here, however, the structure of the terms in Eq. (50) limits the allowed interchanges. The Ψ coefficient in $\mathcal{U}^{(4)}$, for example, will stay the same for an interchange of **1** and **2**, or **3** and **4**, but not for an interchange of **1** and **3**, etc. This is the reason for the grouping of indices in $\Psi_{\mathbf{12},\mathbf{34}}$ and $\Phi_{\mathbf{123},\mathbf{4}}$. This notation is used to indicate that any sequence of indices that occur without a comma can be interchanged without affecting the Hamiltonian. This selective interchangeability plays an important role in the algebraic development of explicit results given below.

Equations (37), (39), (43), (48), and (50), together with accompanying definitions of the coefficients comprise a complete and general statement of the Hamiltonian function up to the fourth order in the spin-wave amplitudes $a_{\mathbf{k}}$ and $a_{\mathbf{k}}^*$. Along with the Hamiltonian equations of motion in Eq. (8) for the spin-wave amplitudes they represent a complete formulation of spin-wave dynamics for a homogeneous sample

under the two conditions noted above: (i) that the energy can be written as a quadratic functional of magnetization, as in Eq. (9), and (ii) that the system self-field $\mathbf{H_M}(\mathbf{r}, t)$ can be written as a linear plane-wave expansion with respect to the magnetization, as in Eq. (26).

V. TRANSFORMATION OF THE HAMILTONIAN FUNCTION TO LINEAR NORMAL MODES

The above development gives a complete statement of the spin-wave dynamics Hamiltonian up to fourth order in the canonical spin-wave amplitudes. The obvious algebraic complexity, however, precludes the application of this raw Hamiltonian to practical calculations. Two further transformations lead to a much simpler form that yields important practical results in both linear and nonlinear spin-wave dynamics. The first transformation is a linear transformation, well known in the literature as the HP transformation. This transformation and its impact on the structure of $\mathcal{U}$ up to fourth order is the focus of this section. The second transformation is a nonlinear transformation that is needed to further simplify the formalism for the treatment of four-wave processes under certain conditions. This special case will be considered in detail in Sec. VI.

The main purpose of the HP transformation is to reduce second-order Hamiltonian $\mathcal{U}^{(2)}$ term to diagonal form. In this process, the original $a_{\mathbf{k}}$ and $a_{\mathbf{k}}^*$ amplitudes are transformed to a set of normal mode spin-wave amplitudes, taken here as $b_{\mathbf{k}}$ and $b_{\mathbf{k}}^*$. The result is a simple second-order Hamiltonian term of the form $\mathcal{U}^{(2)} = \Sigma_{\mathbf{k}} \omega_{\mathbf{k}} b_{\mathbf{k}}^* b_{\mathbf{k}}$, where $\omega_{\mathbf{k}}$ is the eigenfrequency of the spin-wave normal mode at wave vector $\mathbf{k}$. The recipe for this reduction was given in the seminal paper by Holstein and Primakoff in 1941.[60] Once this transformation is established, one can then recast the remaining dynamic terms in $\mathcal{U}$, namely, $\mathcal{U}^{(1)}$, $\mathcal{U}^{(3)}$, and $\mathcal{U}^{(4)}$, in terms of the $b_{\mathbf{k}}$ and $b_{\mathbf{k}}^*$ as well. Insofar as $\mathcal{U}^{(0)}$ contains only constant terms and has no $a_{\mathbf{k}}$ or $a_{\mathbf{k}}^*$ factors, the HP transformation has no effect on this zeroth-order component in $\mathcal{U}$. From the nature of the terms in $\mathcal{U}^{(3)}$ and $\mathcal{U}^{(4)}$ as tabulated above, the reader can see that this operation, while straightforward, is algebraically tedious.

The change over to the normal modes associated with $\mathcal{U}^{(2)}$ provides a working basis for many linear problems in spin-wave dynamics and the realization of the appropriate spin-wave dispersion relation for $\omega_{\mathbf{k}}$. The more powerful application, however, is for nonlinear spin-wave dynamics. Explicit expressions for $\mathcal{U}^{(3)}$ and $\mathcal{U}^{(4)}$ in the $(b_{\mathbf{k}}, b_{\mathbf{k}}^*)$ amplitudes correspond to a nonlinear perturbation to the linear spin-wave dynamics embodied in $\mathcal{U}^{(2)}$. The expressions for $\mathcal{U}^{(3)}$ and $\mathcal{U}^{(4)}$ in terms of the $b_{\mathbf{k}}$ and $b_{\mathbf{k}}^*$ also provide working basis for the further analysis of four-wave processes alluded to above.

Recall the Case I analysis in the development of $\mathcal{U}^{(2)}$ in Sec. IV C. For this case, the z component of the external field was taken as spatially homogeneous and time independent. This limit gave a relatively simple form for $\mathcal{U}^{(2)}$ that couples modes with wave vectors $\mathbf{k}$ and $-\mathbf{k}$ only, as given in Eq. (44). In essence, this nondiagonal form yields equations of motion for coupled harmonic oscillators represented by spin-wave amplitudes $a_{\mathbf{k}}$ and $a_{-\mathbf{k}}^*$. The HP transformation serves to decouple these modes. For the present purposes, the HP transformation is written here as[41,60]

$$\begin{bmatrix} a_\mathbf{k}(t) \\ a_{-\mathbf{k}}^*(t) \end{bmatrix} = \begin{pmatrix} u_\mathbf{k} & v_\mathbf{k} \\ v_\mathbf{k}^* & u_\mathbf{k} \end{pmatrix} \cdot \begin{bmatrix} b_\mathbf{k}(t) \\ b_{-\mathbf{k}}^*(t) \end{bmatrix}. \tag{53}$$

The $u_\mathbf{k}$ and $v_\mathbf{k}$ are given by

$$u_\mathbf{k} = \sqrt{\frac{A_\mathbf{k} + \omega_\mathbf{k}}{2\omega_\mathbf{k}}} \tag{54}$$

and

$$v_\mathbf{k} = -\frac{B_\mathbf{k}}{|B_\mathbf{k}|} \sqrt{\frac{A_\mathbf{k} - \omega_\mathbf{k}}{2\omega_\mathbf{k}}} \tag{55}$$

with a spin-wave frequency

$$\omega_\mathbf{k} = \sqrt{A_\mathbf{k}^2 - |B_\mathbf{k}|^2}. \tag{56}$$

Equation (56) gives the general $\omega_\mathbf{k}$ vs $\mathbf{k}$ dispersion relation for the linear normal mode excitations associated with these amplitudes. Specific expressions for $\omega_\mathbf{k}(\mathbf{k})$ for different physical magnetic systems have found extensive use in the decades since the discovery of FMR and spin-wave resonance phenomena in ferrites, thin films, etc. Details of the HP transformation are given in Refs. 53 and 62, among others. Recall that the $A_\mathbf{k}$ and $B_\mathbf{k}$ are both fully defined in terms of the magnetization of the material, the different components of the effective spin-wave tensor $\mathbf{N}_\mathbf{k}$, and the static internal field, as given in Eqs. (30) and (45), respectively.

Recall from Sec. III D that $\mathbf{N}_\mathbf{k}$ is equal to $\mathbf{N}_{-\mathbf{k}}$ and its components are real. These properties propagate to the $A_\mathbf{k}$ and $B_\mathbf{k}$ as well. It follows that (i) $A_\mathbf{k}$ and $u_\mathbf{k}$ are real and (ii) the conditions $u_\mathbf{k} = u_{-\mathbf{k}}$, $v_\mathbf{k} = v_{-\mathbf{k}}$, and $\omega_\mathbf{k} = \omega_{-\mathbf{k}}$ are satisfied. In terms of $b_\mathbf{k}$, $b_\mathbf{k}^*$ variables, $\mathcal{U}^{(2)}$ takes the diagonal normal-mode form alluded to above

$$\mathcal{U}^{(2)} = \sum_\mathbf{k} \omega_\mathbf{k} b_\mathbf{k}^*(t) b_\mathbf{k}(t). \tag{57}$$

Since the HP transformation is canonical, the equations of motion for the $b_\mathbf{k}$ and $b_\mathbf{k}^*$ amplitudes retain the Hamiltonian form developed in Sec. II and given by Eq. (8). Physically, the HP transformation corresponds to a change over from generally elliptically polarized spin-wave modes $a_\mathbf{k}$ and $a_{-\mathbf{k}}^*$ to circularly polarized modes $b_\mathbf{k}$ and $b_{-\mathbf{k}}^*$. The special case when $B_\mathbf{k}$ is zero corresponds to circularly polarized $a_\mathbf{k}$ and $a_{-\mathbf{k}}^*$ modes. Reference 62 provides a tutorial discussion of this property.

With the HP transformation as given in Eq. (53) now established, one can proceed to the development of $\mathcal{U}^{(1)}$, $\mathcal{U}^{(3)}$, and $\mathcal{U}^{(4)}$ in terms of the $b_\mathbf{k}$ and $b_\mathbf{k}^*$. The transformation of $\mathcal{U}^{(1)}$ term is straightforward and leads to

$$\mathcal{U}^{(1)} = -\sum_\mathbf{k} [u_\mathbf{k} F_\mathbf{k}^*(t) + v_\mathbf{k}^* F_{-\mathbf{k}}(t)] b_\mathbf{k}(t) + \text{c.c.} \tag{58}$$

The $F_\mathbf{k}(t)$ coefficient is the same as given in Eq. (40). As noted in Sec. IV, in the limit of uniform mode dynamics only, $F_\mathbf{k}(t)$ reduces to a simple transverse field pumping term only, with the form $|\gamma| h_{\perp,0}(t)$. This is the driving term in standard uniform mode FMR situations.

The transformation of $\mathcal{U}^{(3)}$ is more involved. For sake of simplicity, $\mathcal{U}^{(3)}$ will be taken in the form given in Eq. (49) for the special case of no external transverse field, that is,

$H_{\perp,\mathbf{k}} = 0$. This case will be important for the development of four-wave coupling coefficients in Secs. VI and VII. The change over from the $a_\mathbf{k}$ and $a_\mathbf{k}^*$ to the $b_\mathbf{k}$ and $b_\mathbf{k}^*$ amplitudes is basically a problem of tabulation that is straightforward but tedious. The transformed third-order Hamiltonian term takes the form

$$\mathcal{U}^{(3)} = \frac{1}{3} \sum_{123} [U_{123}^* b_1(t) b_2(t) b_3(t) + \text{c.c.}] \Delta(\mathbf{1 + 2 + 3})$$
$$+ \sum_{123} [V_{12,3}^* b_1(t) b_2(t) b_3^*(t) + \text{c.c.}] \Delta(\mathbf{1 + 2 - 3}) \tag{59}$$

with coefficients

$$U_{123} = -\frac{1}{2} [(D_1 u_1 + D_1^* v_1)(u_2 v_3 + v_2 u_3) + (D_2 u_2 + D_2^* v_2)(u_1 v_3 + v_1 u_3) + (D_3 u_3 + D_3^* v_3)(u_1 v_2 + v_1 u_2)] \tag{60}$$

and

$$V_{12,3} = -\frac{1}{2} [(D_1 u_1 + D_1^* v_1)(u_2 u_3 + v_2 v_3^*) + (D_2 u_2 + D_2^* v_2) \times (u_1 u_3 + v_1 v_3^*) + (D_3^* u_3 + D_3 v_3^*)(u_1 v_2 + v_1 u_2)]. \tag{61}$$

Following the notation set up earlier, the (**1,2,3**) etc. nomenclature refers to different $\mathbf{k}$ values. Note that for a circular spin-wave polarization, that is, for $u_\mathbf{k} = 1$ and $v_\mathbf{k} = 0$ for all $\mathbf{k}$ values, one obtains $U_{123} = 0$ and $V_{12,3} = -(D_1 + D_2)/2$, in agreement with Eq. (49). As with previous coefficients, the specific U_{123} and $V_{12,3}$ forms mean that only the sequences $\mathbf{k}$ subscripts without a comma separator may be interchanged at will.

The transformed fourth-order Hamiltonian term takes the form

$$\mathcal{U}^{(4)} = \frac{1}{2} \sum_{1234} W_{12,34} b_1(t) b_2(t) b_3^*(t) b_4^*(t) \Delta(\mathbf{1 + 2 - 3 - 4})$$
$$+ \sum_{1234} [G_{123,4}^* b_1(t) b_2(t) b_3(t) b_4^*(t) + \text{c.c.}] \Delta(\mathbf{1 + 2 + 3} - \mathbf{4}) + \frac{1}{4} \sum_{1234} [R_{1234}^* b_1(t) b_2(t) b_3(t) b_4(t) + \text{c.c.}]$$
$$\times \Delta(\mathbf{1 + 2 + 3 + 4}) \tag{62}$$

with expansion coefficients

$$W_{12,34} = \Psi_{12,(-3)(-4)}(u_1 u_2 u_3 u_4 + v_1^* v_2^* v_3 v_4) + \Psi_{2(-3),1(-4)}$$

$$\times (u_1 v_2^* u_3 v_4 + v_1^* u_2 v_3 u_4) + \Psi_{1(-3),2(-4)}(u_1 v_2^* v_3 u_4$$

$$+ v_1^* u_2 u_3 v_4) + \Phi_{123,4} v_1^* v_2^* v_3 v_4 + \Phi_{123,4}^* u_1 u_2 u_3 u_4$$

$$+ \Phi_{412,3} v_1^* v_2^* v_3 u_4 + \Phi_{412,3}^* u_1 u_2 u_3 v_4 + \Phi_{341,2} v_1^* u_2 u_3 u_4$$

$$+ \Phi_{341,2}^* u_1 v_2^* v_3 v_4 + \Phi_{234,1} u_1 v_2^* u_3 u_4 + \Phi_{234,1}^* v_1^* u_2 v_3 v_4,$$

$$(63)$$

$$G_{123,4} = \frac{1}{3}[\Psi_{12,3(-4)}(u_1 u_2 v_3 u_4 + v_1 v_2 u_3 v_4^*) + \Psi_{23,1(-4)}$$

$$\times (v_1 u_2 u_3 u_4 + u_1 v_2 v_3 v_4^*) + \Psi_{13,2(-4)}(u_1 v_2 u_3 u_4$$

$$+ v_1 u_2 v_3 v_4^*) + \Phi_{123,4} u_1 u_2 u_3 u_4 + \Phi_{123,4}^* v_1 v_2 v_3 v_4^*$$

$$+ \Phi_{412,3} u_1 u_2 v_3 v_4^* + \Phi_{412,3}^* v_1 v_2 u_3 u_4 + \Phi_{341,2} u_1 v_2 u_3 v_4^*$$

$$+ \Phi_{341,2}^* v_1 u_2 v_3 u_4 + \Phi_{234,1} v_1 u_2 u_3 v_4^* + \Phi_{234,1}^* u_1 v_2 v_3 u_4]$$

$$(64)$$

and

$$R_{1234} = \frac{1}{3}[\Psi_{12,34}(u_1 u_2 v_3 v_4 + v_1 v_2 u_3 u_4) + \Psi_{23,14}(u_1 v_2 v_3 u_4$$

$$+ v_1 u_2 u_3 v_4) + \Psi_{13,24}(u_1 v_2 u_3 v_4 + v_1 u_2 v_3 u_4)$$

$$+ \Phi_{123,4} u_1 u_2 u_3 v_4 + \Phi_{123,4}^* v_1 v_2 v_3 u_4 + \Phi_{412,3} u_1 u_2 v_3 u_4$$

$$+ \Phi_{412,3}^* v_1 v_2 u_3 v_4 + \Phi_{341,2} u_1 v_2 u_3 u_4 + \Phi_{341,2}^* v_1 u_2 v_3 v_4$$

$$+ \Phi_{234,1} v_1 u_2 u_3 u_4 + \Phi_{234,1}^* u_1 v_2 v_3 v_4].$$

$$(65)$$

Note that the sum terms with the W coefficients have no complex conjugate add-ons. This means that the individual terms in this sum will be, in general, complex. It is easy to see from the structure of Eq. (63) that $W_{12,34} = W_{34,12}^*$ is true, so that this sum term in $\mathcal{U}^{(4)}$ is guaranteed to be real, as required. Notice also that for a circular polarization, that is, for $u_\mathbf{k} = 1$ and $v_\mathbf{k} = 0$, one obtains $W_{12,34} = \Psi_{12,(-3)(-4)}$, $G_{123,4} = \Phi_{123,4}$, and $R_{1234} = 0$, in agreement with Eq. (50). As one additional check on the algebra, one can see that the allowed interchange of indices indicated by the structure of the $W_{12,34}$, $G_{123,4}$, and R_{1234} labels on the left side of Eqs. (63)–(65) carry over consistently to the detailed sequences of terms on the right-hand side of these equations. The right-side expression for R_{1234}, for example, is invariant under any permutation of indices.

VI. ELIMINATION OF NONRESONANT TERMS FROM THE HAMILTONIAN

The new consideration for this section concerns *resonant* and *nonresonant* processes. It is important to keep in mind that the $\mathcal{U}^{(3)}$ and $\mathcal{U}^{(4)}$ terms in the Hamiltonian represent nonlinear interaction processes which destroy certain spin waves and create others. By their very nature, such processes must conserve momentum and energy. In the present classical picture, momentum conservation is already embodied in the Kronecker delta functions that appear in the various $\mathbf{k}$ sums in the equations developed above. The $V_{12,3}$ and $V_{12,3}^*$ terms

in $\mathcal{U}^{(3)}$, for example, contains a $\Delta(1+2-3)$ factor, with the corresponding implied momentum conservation condition, $\mathbf{k}_1 + \mathbf{k}_2 = \mathbf{k}_3$. The companion energy conservation condition is given as $\omega_1 + \omega_2 = \omega_3$. The energy conservation is not explicitly embodied in the classical form of the equations but is generally clear from the actual mode responses. If the physical configuration of the problem at hand in terms of field, sample geometry, sample parameters, etc., allow these momentum and energy conservation conditions to be satisfied, the processes are taken as resonant. If the situation is such that these conditions cannot be satisfied, the corresponding processes are taken as nonresonant.

As an example, resonant three-wave interactions of the form $\mathbf{1} \rightarrow (\mathbf{2}, \mathbf{3})$ correspond to the well-known situation of Suhl first-order spin-wave instability. In this situation, one pumped magnon, typically at $\mathbf{k} \approx 0$, splits into two half frequency magnons with equal and opposite $\mathbf{k}$ vectors. Such processes give rise to the well-known subsidiary absorption loss peak in ferromagnetic resonance. The ferromagnetic resonance response for a sufficiently high field or frequency often corresponds to the case for which such three-wave $\mathbf{1} \rightarrow (\mathbf{2}, \mathbf{3})$ type processes are not allowed and the experimental resonance saturation response is controlled mainly by four-wave processes of the form $(\mathbf{1}, \mathbf{2}) \rightarrow (\mathbf{3}, \mathbf{4})$ that is described by the $W_{12,34}$ sum terms in $\mathcal{U}^{(4)}$.

Section VII will consider two special cases of $(\mathbf{1}, \mathbf{2}) \rightarrow (\mathbf{3}, \mathbf{4})$ processes that are relevant to current nonlinear spin-wave dynamics problems. Case A in Sec. VII corresponds to scattering interactions of the form $(0, 0) \rightarrow (\mathbf{k}, -\mathbf{k})$. This case represents the classic situation for second-order spin-wave instability or resonance-saturation processes. This process, first described theoretically by Harry Suhl in the 1950s,[34] is extremely important for many problems in nonlinear dynamics of current interest, including magnetization reversal in thin magnetic films,[54] and spin torque,[63,64] for example. Case B corresponds to processes of the form $(\mathbf{k}, \mathbf{k}) \rightarrow (\mathbf{k}, \mathbf{k})$. Such a nonlinear self interaction for spin waves with a common wave vector is always resonant. These processes are of direct relevance to any problem in nonlinear spin-wave dynamics in which the frequency shift associated with the pumped spin-wave modes is important. This includes microwave magnetic soliton dynamics[65] and spin torque oscillators.[56,66]

Under typical situations for which these four-wave processes come into play, it turns out that there are no allowed three-wave processes that involve the relevant modes. It also turns out, however, that even though three-wave processes are nonresonant, the $\mathcal{U}^{(3)}$ term in the Hamiltonian still plays an important role in the four-wave scattering problem. The way forward in the analysis in this situation is to perform a transformation that eliminates $\mathcal{U}^{(3)}$ from the overall Hamiltonian. The effect of this transformation is to fold in the three-wave coefficients into a modified $\mathcal{U}^{(4)}$ Hamiltonian term. The focus here is on this procedure and its ramifications.

It is important to emphasize at the outset that this subtle but critical point is not well appreciated. In the initial work by Suhl[34] and Schlömann,[39] for example, the problem of FMR saturation at high microwave power levels was analyzed in terms of "bare" four-wave processes as embodied in the $\mathcal{U}^{(4)}$ term in the Hamiltonian developed above. Their re-

sults for the threshold microwave field amplitude of the resonance saturation spin-wave instability turned out to be correct for one simple reason, namely, that the critical spin-wave modes obtained from the analysis were such as to make the correction terms from $\mathcal{U}^{(3)}$ vanish. This fortuitous situation applies to the threshold power for resonance saturation but not for the general steady-state response above threshold. The importance of nonresonant three-wave terms in general for four-wave scattering processes was first pointed out by Zakharov.[58] Livesey *et al.*[55] have recently applied this type of analysis to large-angle nonlinear spin-wave dynamics in thin films.

Details on the transformation and the logical steps for its development may be found in the highly cogent report by Krasitskii.[67] Note, however, that Ref. [67] considers only a Hamiltonian function for which all expansion coefficients are real. In general, and for the cases of interest here, the Hamiltonian coefficients are complex. The Krasitskii development still applies but it is necessary to go through the full analysis with this change in mind. A full step-by-step development is beyond the scope of this paper and only the final results are given below.

Keep in mind that there have already been three transformations, the original Schlömann transformation from the vector magnetization $\mathbf{M}(\mathbf{r},t)$ to the scalar $a(\mathbf{r},t)$ and $a^*(\mathbf{r},t)$ canonical variables, the further canonical transformation to the $a_{\mathbf{k}}(t)$ and $a_{\mathbf{k}}^*(t)$ spin-wave amplitudes, and then the HP transformation to the $b_{\mathbf{k}}(t)$ and $b_{\mathbf{k}}^*(t)$ amplitudes that diagonalizes the second-order $\mathcal{U}^{(2)}$ term in the Hamiltonian and yield the normal modes for the linear problem. The transformation of interest here carries the $b_{\mathbf{k}}$ and $b_{\mathbf{k}}^*$ over to new spin-wave amplitudes $c_{\mathbf{k}}$ and $c_{\mathbf{k}}^*$ that eliminate the $\mathcal{U}^{(3)}$ term from the Hamiltonian. This transformation is valid only under the nonresonant conditions discussed above. Following the Krasitskii approach, this transformation takes the form of power series that can be written as

$$b_{\mathbf{k}}(t) = c_{\mathbf{k}}(t) - \sum_{12} \left\{ \frac{V_{12,\mathbf{k}}^*}{\omega_{\mathbf{k}} - \omega_1 - \omega_2} c_1(t)c_2(t)\Delta(\mathbf{k}-\mathbf{1}-\mathbf{2}) \right.$$

$$+ 2\frac{V_{1\mathbf{k},2}}{\omega_{\mathbf{k}} + \omega_1 - \omega_2} c_1(t)c_2^*(t)\Delta(\mathbf{k}+\mathbf{1}-\mathbf{2})$$

$$\left. + \frac{U_{12\mathbf{k}}}{\omega_{\mathbf{k}} + \omega_1 + \omega_2} c_1^*(t)c_2^*(t)\Delta(\mathbf{k}+\mathbf{1}+\mathbf{2}) \right\}. \quad (66)$$

While the algebra is rather tedious, the Hamiltonian in terms of the $c_{\mathbf{k}}$ and $c_{\mathbf{k}}^*$ can be obtained as

$$\mathcal{U} = \sum_{\mathbf{k}} \omega_{\mathbf{k}} c_{\mathbf{k}}^*(t)c_{\mathbf{k}}(t) + \frac{1}{2}\sum_{1234} \widetilde{W}_{12,34} c_1(t)c_2(t)c_3^*(t)c_4^*(t)\Delta(\mathbf{1}+\mathbf{2}$$

$$-\mathbf{3}-\mathbf{4}) + \text{remaining fourth order(RFO)terms.} \quad (67)$$

One can see that the leading second order $\mathcal{U}^{(2)}$ term in the Hamiltonian and the normal mode spin-wave frequency $\omega_{\mathbf{k}}$ are not affected by the transformation to $c_{\mathbf{k}}$ and $c_{\mathbf{k}}^*$ amplitudes. The $\widetilde{W}_{12,34}$ represent renormalized versions of the $W_{12,34}$ coefficients for $(\mathbf{1},\mathbf{2})\rightarrow(\mathbf{3},\mathbf{4})$ process. Expanded expressions for the $\widetilde{W}_{12,34}$ will be considered shortly. The re-

maining fourth-order (RFO) terms correspond to $(\mathbf{1})\rightarrow(\mathbf{2},\mathbf{3},\mathbf{4})$, etc., processes. Comments on these terms are given at the end of the section. In principle, the $\mathcal{U}^{(1)}$ term given in Eq. (58) carries over to the new Hamiltonian but now expressed in terms of the $c_{\mathbf{k}}$ and $c_{\mathbf{k}}^*$. For simplicity, this term is not included in Eq. (67) as it has no effect on the nonlinear dynamics to be considered in Sec. VII.

The general form of the $\widetilde{W}_{12,34}$ coefficients for unrestricted sets of the four eigenfrequencies ω_1 through ω_4 is quite complicated and of no direct interest here. Reference 67 does provide formulas for these terms in the case of a Hamiltonian with real coefficients. Recall, however, that for the specific $(\mathbf{1},\mathbf{2})\rightarrow(\mathbf{3},\mathbf{4})$ processes of interest here, one has large amplitudes only if the resonance condition

$$\omega_1 + \omega_2 = \omega_3 + \omega_4 \quad (68)$$

is satisfied. In this special case, the $\widetilde{W}_{12,34}$ take a simple additive form written here as

$$\widetilde{W}_{12,34} = W_{12,34} + T_{12,34} \quad (69)$$

with the $T_{12,34}$ given by

$$T_{12,34} = -2\left[\frac{U_{12(-1-2)}^* U_{34(-3-4)}}{\omega_{-1-2} + \omega_1 + \omega_2} + \frac{V_{12,(1+2)}^* V_{34,(3+4)}}{\omega_{3+4} - \omega_3 - \omega_4} \right.$$

$$+ \frac{V_{2(4-2),4}^* V_{3(1-3),1}}{\omega_{1-3} + \omega_3 - \omega_1} + \frac{V_{1(3-1),3}^* V_{4(2-4),2}}{\omega_{2-4} + \omega_4 - \omega_2}$$

$$\left. + \frac{V_{2(3-2),3}^* V_{4(1-4),1}}{\omega_{1-4} + \omega_4 - \omega_1} + \frac{V_{1(4-1),4}^* V_{3(2-3),2}}{\omega_{2-3} + \omega_3 - \omega_2} \right]. \quad (70)$$

The $T_{12,34}$ represents the effect of the nonresonant three-wave processes, now transformed out of the Hamiltonian, to the resonant four-wave $(\mathbf{1},\mathbf{2})\rightarrow(\mathbf{3},\mathbf{4})$ process. The various U and V parameters carry over from the now eliminated $\mathcal{U}^{(3)}$ term in the Hamiltonian and were defined in Eqs. (60) and (61). As with $W_{12,34}$, it is easy to see from Eq. (70) that $T_{12,34} = T_{34,12}^*$ is true so that $\mathcal{U}^{(4)}$ is guaranteed to be real, as required.

Even though the $T_{12,34}$ expression is rather complicated, its physical basis can be understood in a simple way. Recall that the U and V coefficients in $\mathcal{U}^{(3)}$ represent the amplitudes for specific three-wave scattering process. The U_{123} and U_{123}^* in Eq. (59), for example, represent scattering amplitudes for processes in which three spin waves $\mathbf{k}_1$, $\mathbf{k}_2$, and $\mathbf{k}_3$ are created or destroyed respectively. This means that the leading $U_{12(-1-2)}^* U_{34(-3-4)}$ term in $T_{12,34}$ represents processes in which spin waves with $\mathbf{k}_1$, $\mathbf{k}_2$, and $\mathbf{k}=-\mathbf{k}_1-\mathbf{k}_2$ are destroyed and additional spin waves with $\mathbf{k}_3$, $\mathbf{k}_4$, and $\mathbf{k}'=-\mathbf{k}_3-\mathbf{k}_4$ are created. The $\Delta(\mathbf{1}+\mathbf{2}-\mathbf{3}-\mathbf{4})$ constraint in Eq. (67), however, means that $\mathbf{k}$ is equal to $\mathbf{k}'$, so that the combined result of these two three-wave processes corresponds to a single $(\mathbf{1},\mathbf{2})\rightarrow(\mathbf{3},\mathbf{4})$ four-wave process. Note also that the $\omega_{-1-2} + \omega_1 + \omega_2$ denominator that accompanies this term in $T_{12,34}$ mirrors this same overall process.

Similar connections apply for the remaining terms in Eq. (70). Consider the $V_{12,(1+2)}^* V_{34,(3+4)}$ product, for example. The $V_{12,(1+2)}^*$ part corresponds to the situation in which spin
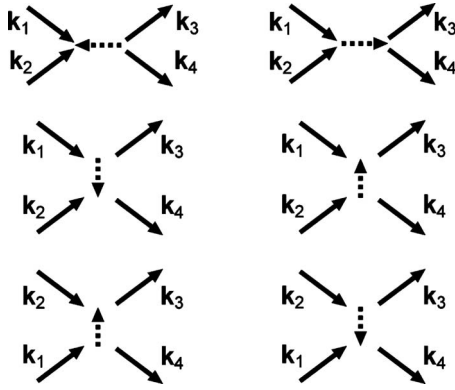
FIG. 1. Graphical representation of the six explicit $(\mathbf{1},\mathbf{2}) \rightarrow (\mathbf{3},\mathbf{4})$ four-wave scattering processes described by the six terms in $T_{\mathbf{12,34}}$ from Eq. (70). The solid arrows represent the spin-wave modes involved in $(\mathbf{1},\mathbf{2}) \rightarrow (\mathbf{3},\mathbf{4})$ process. The dashed arrows represent the intermediate nonresonant three-wave scattering processes that make up the actual interactions. The relative positions of the diagrams mirror the layout of terms in Eq. (70).

waves with $\mathbf{k}_1$ and $\mathbf{k}_2$ are destroyed and a spin wave with $\mathbf{k} = \mathbf{k}_1 + \mathbf{k}_2$ is created. The $V_{\mathbf{34,(3+4)}}$ part corresponds to the situation in which spin waves with $\mathbf{k}' = \mathbf{k}_3 + \mathbf{k}_4$ are destroyed and spin waves with $\mathbf{k}_3$ and $\mathbf{k}_4$ are created. As before, the $\mathbf{k} = \mathbf{k}'$ condition transforms these sequential three-wave processes in to a single $(\mathbf{1},\mathbf{2}) \rightarrow (\mathbf{3},\mathbf{4})$ four-wave process. The $\omega_{\mathbf{3+4}} - \omega_{\mathbf{3}} - \omega_{\mathbf{4}}$ denominator mirrors this process as well. In this case, however, the in-out nature of the individual three-wave interactions is also mirrored by the explicit form as an energy difference. It is important to keep in mind that the entire analysis of this section is for nonresonant three-wave processes. This means that none of the denominators in Eq. (70) can ever vanish and, in general, will be on the order of the spin-wave frequencies themselves. For the simple case for which $\mathbf{k}_1 = \mathbf{k}_2 = \mathbf{k}_3 = \mathbf{k}_4 = 0$ is satisfied, the denominators for the terms in Eq. (70) reduce to $3\omega_0$ for the first term and $\pm\omega_0$ for the others. Insofar as these all amount to scattering parameters, a sign change simply denotes a change in phase.

Figure 1 provides a graphical depiction of the various $(\mathbf{1},\mathbf{2}) \rightarrow (\mathbf{3},\mathbf{4})$ scattering processes for the six terms in the $T_{\mathbf{12,34}}$ expression of Eq. (70) coefficient. The positions of the diagrams mirror the layout of terms in Eq. (70). The left- and right-side solid arrows represent the $(\mathbf{1,2})$ spin-wave pairs that are destroyed and the $(\mathbf{3,4})$ spin-wave pairs that are created in each of the six hybrid interactions, respectively. The dashed arrows that connect these "in" and "out" products represent the matching out and in parts of the individual three-wave terms, in the spirit of the details given above for the first two terms. The dashed arrow in the upper-left diagram, for example, corresponds to either $\mathbf{k} = -\mathbf{k}_1 - \mathbf{k}_2$ or $\mathbf{k}' = -\mathbf{k}_3 - \mathbf{k}_4$. It is reassuring to see that the large amount of algebraic work needed to obtain Eq. (70) actually leads to the only six physical terms that yield four-wave $(\mathbf{1},\mathbf{2}) \rightarrow (\mathbf{3},\mathbf{4})$-type scattering from a combination of two three-wave processes that satisfy the momentum conservation condition $\mathbf{k}_1 + \mathbf{k}_2 = \mathbf{k}_3 + \mathbf{k}_4$. There are no others.

The final remarks for this section concern the labeled but not specified RFO terms in Eq. (67). In principle, these terms

can be also eliminated from the Hamiltonian if the transformation of Eq. (66) is expanded to include cubic terms in the $c_{\mathbf{k}}$ and $c_{\mathbf{k}}^*$ variables.[67] Such a procedure would be even more complicated than the analysis just described. For the problems of interest here, however, these RFO terms play no significant role. This can be seen from the form of these terms. Keep in mind that the $c_{\mathbf{k}}$ take the form $c_{\mathbf{k}}(t) \approx |c_{\mathbf{k}}(t)| e^{-i\omega_{\mathbf{k}}t}$, where $|c_{\mathbf{k}}(t)|$ corresponds to a slowly varying envelope response to be determined from the final equation of motion analysis. For the explicitly stated $(\mathbf{1},\mathbf{2}) \rightarrow (\mathbf{3},\mathbf{4})$ terms in Eq. (67), for example, the different $c_{\mathbf{k}}$ and $c_{\mathbf{k}}^*$ amplitudes occur in pairs. The energy conservation requirement in Eq. (68) means that there will be no surviving high-frequency oscillation response from these terms. For the RFO terms, in contrast, the frequency dependences do not cancel out and the net result is a fourth-order product of spin-wave amplitudes with a high-frequency oscillation type response. A $(\mathbf{1}) \rightarrow (\mathbf{2},\mathbf{3},\mathbf{4})$ term, for example, will lead to a $c_{\mathbf{k}}$ product that varies as $e^{2i\omega_2 t}$. The evolution of the nonlinear response of the spin-wave system, however, is normally described by the *slowly varying envelope functions* noted above and such fast oscillation terms can be typically neglected.

VII. THEORY APPLICATIONS

As indicated above, the application focus of this section is on resonant four-wave $(\mathbf{1},\mathbf{2}) \rightarrow (\mathbf{3},\mathbf{4})$ scattering processes in situations for which three-wave processes are nonresonant. In spite of the physical connections implicit in the general $\widetilde{W}_{\mathbf{12,34}}$ factors discussed above, these factors for the case of four "unconstrained" wave vectors are not particularly useful for practical calculations. "Unconstrained" is shown in quotes because $\mathbf{k}_1$, $\mathbf{k}_2$, $\mathbf{k}_3$, and $\mathbf{k}_4$ are still subject to the momentum and energy conservation requirements discussed above. This section serves to narrow the focus even further, to two specific nonlinear spin-wave problems of fundamental and practical interest. Section I will develop new formulas for the coupling coefficients for Suhl second-order spin-wave instability processes. The working equations will be developed here for the case of a bulk sample in the form of an ellipsoid of revolution. This is the same classical problem analyzed by Suhl[34] and Schlömann,[39] for example, in connection with the nonlinear FMR saturation response in ferrite samples. These seminal papers, however, do not include the effect of the nonresonant three-wave process terms developed in Sec. VI. As will be shown shortly, this three-wave correction can become important under certain conditions.

Section VII B will then consider the nonlinear spin-wave frequency shift in a thin magnetic film. In addition to the critical importance of this parameter for microwave magnetic envelope solitons,[65] the nonlinear frequency shift is central to a proper analysis of the magnetization dynamics for spin momentum transfer in thin-film structures and the emerging class of spin torque oscillator devices.[32,64,68] Among other things, this shift controls the Q factor of the spin torque oscillator response.[56]

To date, however, there has been no completely satisfactory theoretical development of this nonlinear frequency shift. Many workers have adopted a heuristic approach based

on the Kittel FMR equation or linear spin-wave dispersion equations with the saturation magnetization M_s replaced simply by the time-averaged magnetization component along the internal field direction.[69–71] The major problem with this approach is that the starting expressions for the mode frequencies come exclusively from a linear analysis. From the very start, this approach ignores the nonlinear terms in the dynamical equations that are central to a proper analysis. As will be shown shortly, this heuristic approach can often lead to significant errors.

There have also been a number of published results based on a nonlinear spin-wave dynamics approach of the sort developed here.[72–74] The problem with these analyses is threefold. (1) Some of these published works are not fully developed and give abstract results that are of limited practical use. (2) Others appear to contain piecemeal developments and typographical errors or other problems that reduce the credibility of the final cited working equations. (3) Some of the results do not reduce to those from exact numerical methods in simple limits. It is noteworthy that Slavin and Tiberkevich have recently published consistent results for the special case of in-plane and perpendicularly magnetized thin films with in-plane uniaxial anisotropy.[75]

Because of these earlier problems, most of these previous developments and results are of limited practical use. The analysis given below is done for a specific case of an ultrathin magnetic film with static external field applied under a general angle relative to the film normal. It is shown that a strict application of the Hamiltonian method with the three-wave correction terms included leads to consistent nonlinear frequency-shift results. The final frequency-shift expressions given below, taken together with the fully developed formalism from the previous sections, should provide a self consistent, useful, and practical statement of the nonlinear response for spin waves in magnetic systems that should be useful for workers in the field.

A. Suhl second-order spin-wave instability coupling coefficients revisited

Suhl second-order spin-wave instability processes correspond to a situation in which two uniform-mode ($\mathbf{k}=0$) magnons at the FMR frequency ω_0 split into two oppositely directed $(\mathbf{k},-\mathbf{k})$ magnons with $\omega_{\mathbf{k}}=\omega_0$.[34] These single frequency $(0,0)\rightarrow(\mathbf{k},-\mathbf{k})$ processes are central to many basic nonlinear FMR effects and to a host of microwave magnetic device properties. One key effect concerns the critical uniform mode amplitude, taken as $|c_0|_{\mathrm{crit}}$, at which selected nonzero $\mathbf{k}$ modes will be driven to large amplitudes. The c_0 is the steady state uniform-mode amplitude obtained from the equation-of-motion analysis based on the development of Sec. V or Ref. 59, for example. Insofar as c_0 generally scales with the amplitude of the applied microwave pumping field, taken here as uniform and denoted as h_0, one also obtains the spin-wave instability threshold microwave field amplitude h_{crit} often termed the Suhl threshold.

The classic Suhl analysis gives a concise set of working equations for the spin-wave instability threshold. In the terminology of this paper, the basic relation can be written as
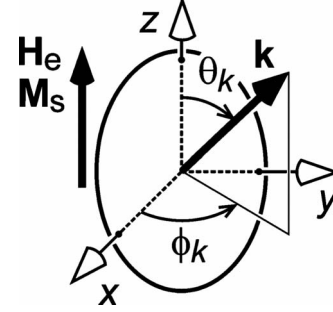

FIG. 2. The sample and the field geometry for the analysis of the Suhl $(0,0)\rightarrow(\mathbf{k},-\mathbf{k})$ coupling coefficient for an isotropic bulk ellipsoidal sample with rotational symmetry. The axis of symmetry is along the z direction. The ellipsoid is magnetized to saturation by the static uniform field $\mathbf{H}_e=H_e\hat{\mathbf{z}}$. The spin-wave mode is defined in terms of the wave vector $\mathbf{k}$ and the corresponding azimuthal and polar propagation angles ϕ_k and θ_k, respectively.

$$|c_0|_{\mathrm{crit}} = \min\left(\sqrt{\frac{\eta_{\mathbf{k}}}{|\widetilde{W}_{00,\mathbf{k}(-\mathbf{k})}|}}\right)_{\omega_{\mathbf{k}}=\omega_0}, \qquad (71)$$

where $\eta_{\mathbf{k}}$ denotes the relaxation rate of a given spin-wave mode and the $\widetilde{W}_{00,\mathbf{k}(-\mathbf{k})}$ is the coupling coefficient for the $(0,0)\rightarrow(\mathbf{k},-\mathbf{k})$ process. The minimization is over all available spin-wave modes at the FMR frequency, as defined through the linear dispersion relation implicit in Eq. (56), for example. In this section, the FMR frequency is always taken equal to the microwave field pumping frequency. In simple terms, one can view the above relation as a power flow equation of the form $\eta_{\mathbf{k}}=|\widetilde{W}_{00,\mathbf{k}(-\mathbf{k})}||c_0|^2_{\mathrm{crit}}$, where $\eta_{\mathbf{k}}$ corresponds to the decay rate of the pumped spin waves at $\pm\mathbf{k}$ and $\omega_{\mathbf{k}}=\omega_0$, and $|\widetilde{W}_{00,\mathbf{k}(-\mathbf{k})}||c_0|^2_{\mathrm{crit}}$ gives the power flow into these modes. The minimization relates to the fact that it is the spin-wave mode with the minimum threshold, so called *critical mode*, that is seen in the experiment experiments.

The purpose of this section is twofold. First, it provides a check on the theory in certain limits for the relatively simple but important and well-known problem of Suhl second-order spin-wave instability threshold. Second, and more importantly, it provides a completely new result for the Suhl coupling coefficient that includes the effect of nonresonant three-wave processes developed in the previous section. As noted, the original developments by Suhl and Schlömann ignored these effects. It is shown that under certain conditions these effects can be important.

For simplicity, the development below is for magnetically isotropic bulk ellipsoidal sample with rotational symmetry. Figure 2 shows the geometry. The axis of symmetry is in the z direction. The ellipsoid is magnetized to saturation by the static uniform field $\mathbf{H}_e=H_e\hat{\mathbf{z}}$. The spin-wave modes are defined in terms of a wave vector $\mathbf{k}$ with azimuthal and polar propagation angles ϕ_k and θ_k, respectively. Following the spirit of the Suhl theory, the spin-wave excitations will be considered in the bulk, short-wavelength limit only. This means that complications due to surface boundary conditions and size effects are avoided.

As with most of the formulas developed above, the specific form of the $\widetilde{W}_{00,\mathbf{k}(-\mathbf{k})}$ coupling coefficient of interest here follows from the various terms in the effective spin-wave tensor $\mathbf{N_k}$. Keep in mind that the general $\widetilde{W}$ coefficient is comprised of two terms, W and T. In this specific case one writes

$$\widetilde{W}_{00,\mathbf{k}(-\mathbf{k})} = W_{00,\mathbf{k}(-\mathbf{k})} + T_{00,\mathbf{k}(-\mathbf{k})}. \quad (72)$$

Each of the terms in $\widetilde{W}_{00,\mathbf{k}(-\mathbf{k})}$ is expressed, in turn, in terms of the various components of the $\mathbf{N_k}$ tensor through a sequence of coefficients as developed in Secs. III–VI. This selected example demonstrates the point made earlier, that the full nonlinear dynamics for a given problem reduces to nothing more than a proper consideration of the starting $\mathbf{N_k}$ tensor.

As in the Suhl approach, it is useful to separate the $\mathbf{N_k}$ solutions for the uniform $\mathbf{k}=0$ mode pumped by the microwave drive and the short-wavelength bulk spin-wave modes with nonzero $\mathbf{k}$ values. The $\mathbf{N_0}$ tensor is the same as the usual the demagnetizing tensor. For the rotationally symmetric sample geometry of Fig. 2 the $\mathbf{N_0}$ is diagonal with $N_{xx,0} = N_{yy,0} = N_\perp$ and $N_{zz,0} = 1 - 2N_\perp$, where $N_\perp$ is the standard transverse demagnetizing factor.

The components of the effective spin-wave $\mathbf{N_k}$ tensor for bulk $\mathbf{k} \neq 0$ spin-wave modes along with an outline of their development are given in Ref. 62, among other sources.

$$N_{xx,\mathbf{k}} = \alpha_{\mathrm{ex}}k^2 + \sin^2\theta_k \cos^2\phi_k.$$

$$N_{yy,\mathbf{k}} = \alpha_{\mathrm{ex}}k^2 + \sin^2\theta_k \sin^2\phi_k.$$

$$N_{zz,\mathbf{k}} = \alpha_{\mathrm{ex}}k^2 + \cos^2\theta_k.$$

$$N_{xy,\mathbf{k}} = N_{yx,\mathbf{k}} = \sin^2\theta_k \sin\phi_k \cos\phi_k.$$

$$N_{xz,\mathbf{k}} = N_{zx,\mathbf{k}} = \sin\theta_k \cos\theta_k \cos\phi_k.$$

$$N_{yz,\mathbf{k}} = N_{zy,\mathbf{k}} = \sin\theta_k \cos\theta_k \sin\phi_k. \quad (73)$$

Note that the exchange term in $\mathbf{N_k}$ is diagonal and isotropic. The form of the dipole terms reflects the spin-wave ellipticity. These specific expressions for the terms in $\mathbf{N_k}$ in combination with Eqs. (30), (45), and (56), lead directly to the well-known bulk spin-wave dispersion relation

$$\omega_{\mathbf{k}} = [(\omega_H + \omega_M \alpha_{\mathrm{ex}}k^2) \times (\omega_H + \omega_M \alpha_{\mathrm{ex}}k^2 + \omega_M \sin^2\theta_k)]^{1/2}. \quad (74)$$

Recall that $\omega_H = |\gamma|H_i$ simply expresses the internal field in frequency units. For the simplified sample geometry at hand, this reduces to $\omega_H = |\gamma|H_e - \omega_M(1 - 2N_\perp)$. For completeness, it is also useful to write down the uniform mode FMR frequency ω_0 that follows from Eqs. (30), (45), and (56) with the terms in $\mathbf{N_0}$ given above.

$$\omega_0 = \omega_H + \omega_M N_\perp = |\gamma|[H_e + 4\pi M_s(N_{zz,0} - N_\perp)]. \quad (75)$$

The bottom line in Eq. (75) is recognizable as the Kittel FMR condition for rotationally symmetric samples. While

Eqs. (74) and (75) will not appear explicitly in the final $\widetilde{W}_{00,\mathbf{k}(-\mathbf{k})}$ expressions given below, they are needed for the development to obtain the cited results.

From the above, one can now obtain working expressions for the two parts of $\widetilde{W}_{00,\mathbf{k}(-\mathbf{k})}$ in Eq. (72). First consider the bare $W_{00,\mathbf{k}(-\mathbf{k})}$ component. For a sample with rotational symmetry, the uniform mode is circularly polarized and one has $u_0 = 1$ and $v_0 = 0$. This leads to a major simplification in the general $W_{00,\mathbf{k}(-\mathbf{k})}$ expression of Eq. (63), and one obtains

$$W_{00,\mathbf{k}(-\mathbf{k})} = \Psi_{00,\mathbf{k}(-\mathbf{k})}u_{\mathbf{k}}^2 + 2\Phi_{00\mathbf{k},\mathbf{k}}^* u_{\mathbf{k}}v_{\mathbf{k}}. \quad (76)$$

Note also that the $u_{\mathbf{k}}$, $v_{\mathbf{k}}$, and $\Phi_{00\mathbf{k},\mathbf{k}}$ coefficients above are even functions with respect to wave vector $\mathbf{k}$ as a consequence of the $\mathbf{N_k} = \mathbf{N_{-k}}$ property discussed in Sec. III. The connections between the terms on the right hand side of Eq. (76) and $\mathbf{N_k}$ were developed in previous sections. With the $\mathbf{N_k}$ components for bulk spin waves from Eq. (73) folded into the analysis, one can obtain $W_{00,\mathbf{k}(-\mathbf{k})}$ in explicit form. One can obtain $W_{00,\mathbf{k}(-\mathbf{k})}$ in a particularly compact form through the use of a simple function given by

$$G_{\pm}(x,q) = \pm 1 + \sqrt{1 + \left(\frac{x}{2q}\right)^2}. \quad (77)$$

In terms of $G_{\pm}(x,q)$, one obtains

$$W_{00,\mathbf{k}(-\mathbf{k})} = \frac{\omega_M q}{4}\left\{\left[G_-(x,q) + \frac{2-3x}{q}\right]G_+(x,q) + \left(\frac{x}{2q}\right)^2\right\} \quad (78)$$

with x taken as $\sin^2\theta_k$ and $q = \omega_0/\omega_M$. There are two important points of note here. First, the rotational symmetry of the problem gives a $W_{00,\mathbf{k}(-\mathbf{k})}$ coefficient that does not depend on the azimuthal spin-wave propagation angle ϕ_k. The second, and more important point, is that the wave-number k dependence of $W_{00,\mathbf{k}(-\mathbf{k})}$ comes in through the $\omega_0 = \omega_{\mathbf{k}}$ constraint. This constraint, in combination with Eqs. (74) and (75) yields the k as a function of $\sin^2\theta_k$ and ω_0, and leads to the relatively simple bare coupling term given in Eq. (78). Note that the $N_\perp$ parameter plays no explicit role in these expressions, apart from its inclusion on the FMR frequency parameter ω_0.

The only equation cited in the literature for comparison with the $W_{00,\mathbf{k}(-\mathbf{k})}$ expression developed above is Eq. (3.49) in the unpublished "R-48" treatise of Schlömann.[39] This R-48 expression, however, is not the same as obtained here. Part of the problem is in a factor of 2 difference in the Hamiltonian convention, and part appears to be due to a typographic error. The computed curves in Fig. 12 of R-48, however, do match the present expression.

The $W_{00,\mathbf{k}(-\mathbf{k})}$ coupling coefficient reduces to an even simpler expression in the high-frequency limit for $\omega_0 \gg \omega_M$. In this limit, one obtains $W_{00,\mathbf{k}(-\mathbf{k})} \approx \omega_M[1 - (3/2)\sin^2\theta_k]$. This simple form directly reflects the nature of the dipole-dipole interactions responsible for the nonlinear coupling. This limiting case is also important for practical applications. In the case of YIG, for example, one has $\omega_M/2\pi \approx 5$ GHz. Many FMR experiments are done at somewhat higher frequencies. In this limit, one can see that the spin-wave modes with

largest $|W_{00,\mathbf{k}(-\mathbf{k})}|$ coupling coefficient are those that propagate along the field direction at $\theta_k=0$. In the original Suhl and Schlömann theory, these $\theta_k=0$ modes with the strongest coupling correspond to the critical modes. With the proper bulk sample uniform mode c_0 expression taken into account, one obtains a simple expression for the linearly polarized microwave field threshold amplitude for spin-wave instability (h_{crit}) equal to $\Delta H(\Delta H_{\mathbf{k}}/4\pi M_s)^{1/2}$, where ΔH is the standard FMR half-power linewidth below threshold and $\Delta H_{\mathbf{k}} = 2\eta_{\mathbf{k}}/|\gamma|$ defines the conventional spin-wave linewidth. This is the famous spin-wave instability threshold field result first developed by Suhl. Traditionally, this is the standard working expression for many practical applications.

Turn now to the new term in the fully developed coupling coefficient, namely, the supplemental $T_{00,\mathbf{k}(-\mathbf{k})}$ three-wave term. As with $W_{00,\mathbf{k}(-\mathbf{k})}$, the specific $(0,0)\rightarrow(\mathbf{k},-\mathbf{k})$ four-wave process considered here results in a major simplification. In addition to the $u_0=1$ and $v_0=0$ conditions noted above, D_0 is also zero. Equations (31), (60), (61), and (70) now combine to yield $T_{00,\mathbf{k}(-\mathbf{k})}$ in a compact form akin to Eq. (78).

$$T_{00,\mathbf{k}(-\mathbf{k})} = -\frac{\omega_M}{2q}x(1-x)\sqrt{G_+(x,q)}\left[\sqrt{G_+(x,q)} - \sqrt{G_-(x,q)}\right]^3.$$

$$(79)$$

The q, x, and $G_\pm$ are the same as before. As above, $N_\perp$ also plays no explicit role in these expressions. From the form of $T_{00,\mathbf{k}(-\mathbf{k})}$, one can see that this three-wave correction term vanishes for θ_k propagation angles of zero and 90°. It also vanishes for the high-frequency limit $\omega_0 \gg \omega_M$. The implications of these properties will be discussed shortly. Based on the expressions in Eqs. (78) and (79), the full $\widetilde{W}_{00,\mathbf{k}(-\mathbf{k})}$ coupling coefficient can now be obtained from Eq. (72).

Graphs (a) and (b) in Fig. 3 summarize the θ_k dependences of the bare $W_{00,\mathbf{k}(-\mathbf{k})}$ and the full $\widetilde{W}_{00,\mathbf{k}(-\mathbf{k})}$ coupling coefficients, respectively. Curves are shown for a range of FMR frequencies, expressed through values of ω_0/ω_M, as indicated. The vertical axes for (a) and (b) show values of W and $\widetilde{W}$, all normalized to ω_M. This scale is reasonable, insofar as the dominant interaction that gives rise to these nonlinear terms is dipole-dipole in nature.

The physical meaning of the curves in Fig. 3 is closely connected to the role of coupling coefficients in defining the Suhl spin-wave instability threshold parameters $|c_0|_{\text{crit}}$ and h_{crit} that were introduced above. For a given FMR frequency and, hence, a given curve in (a) or (b), it is the maximum value of W or $\widetilde{W}$ that will determine the θ_k value for the critical mode. Note that this is true, strictly speaking, only if the spin-wave relaxation rate $\eta_{\mathbf{k}}$, or the equivalent spin-wave linewidth $\Delta H_{\mathbf{k}}$, is wave-vector ($\mathbf{k}$) independent. The situation when these relaxation parameters are wave vector dependent will be considered shortly.

From the curves for the bare $W_{00,\mathbf{k}(-\mathbf{k})}$ parameter in (a) one can see that for frequencies above about $\omega_M/10$ or so, the maximum coupling will occur at $\theta_k=0$. For a $\mathbf{k}$-independent spin-wave linewidth ($\Delta H_{\mathbf{k}}$), these are the critical modes associated with the Suhl result noted above, h_{crit}
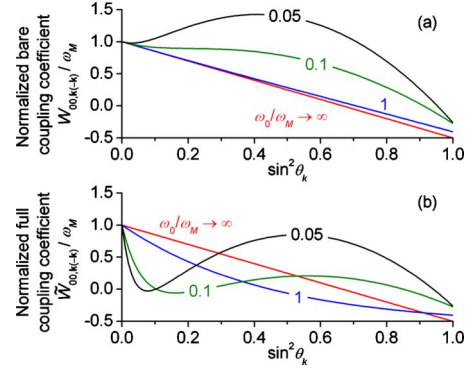

FIG. 3. (Color online) Graphs (a) and (b) show plots of the bare four-wave $W_{00,\mathbf{k}(-\mathbf{k})}$ and the three-wave augmented $\widetilde{W}_{00,\mathbf{k}(-\mathbf{k})}$ coupling coefficients, respectively, as a function of $\sin^2\theta_k$, where θ_k is the polar spin-wave propagation angle. Curves are shown for selected values of the ferromagnetic resonance frequency ω_0, shown in ratio to the magnetization frequency parameter ω_M. The vertical axis W and $\widetilde{W}$ values are also shown in normalized form, relative to ω_M. As a practical calibration, $\omega_M/2\pi$ is about 5 GHz for yttrium iron garnet. All curves are for the $(0,0)\rightarrow(\mathbf{k},-\mathbf{k})$ four-wave scattering scenario for which the spin-wave frequency $\omega_{\mathbf{k}}$ is equal to ω_0.

$=\Delta H(\Delta H_{\mathbf{k}}/4\pi M_s)^{1/2}$. The situation is modified somewhat for lower frequencies, as evident from the topmost curve in (a). One can see that for frequencies below $\omega_M/10$ or so, the development of a peak in the $W(\theta_k)$ profile will serve to select out critical modes at $\theta_k \sim 45°$. The caveat here is that three-wave processes, taken to be forbidden for the purposes of this analysis, can come into play if ω_0/ω_M falls below $2N_\perp$, and this imposes a lower limit on the applicability of the present analysis.

Before moving on to the augmented $\widetilde{W}(\theta_k)$ term shown in (b), it is useful to consider the effect of a $\mathbf{k}$-dependent $\eta_{\mathbf{k}}$ or $\Delta H_{\mathbf{k}}$ on the critical modes in (a). This is because both these relaxation parameters are generally strong functions of the wave number k and the propagation angles θ_k and ϕ_k as well.[15,76–78] Such dependences mean that the maximum value of $|W(\mathbf{k})|/\eta_{\mathbf{k}}(\mathbf{k})$ with respect to $\mathbf{k}$, not just the maximum of $|W(\mathbf{k})|$, will define the Suhl critical modes for a given system. Recall that this maximization, which corresponds to the "min" operation in Eq. (71), is always carried out subject to the $\omega_{\mathbf{k}}=\omega_0$ energy-conservation constraint for the $(0,0)\rightarrow(\mathbf{k},-\mathbf{k})$ four-wave process considered here.

By way of example, consider the three-wave confluence process in which an excited spin-wave mode interacts with thermal magnons. In certain limits, this process gives an $\eta_{\mathbf{k}}$ that varies linearly with k, i.e., of the form $A+Bk$.[76,77] Based on the bulk spin-wave dispersion equation given in Eq. (74), one can see that this type of an $\eta_{\mathbf{k}}(k)$ function will push the critical modes to lower k or higher θ_k values. In the context of Fig. 3(a), this will correspond to a possible shift in the critical modes away from $\theta_k=0$ at high frequencies and to values above the nominal $\theta_k=45°$ limit point at low frequencies. In cases where the B term in $\eta_{\mathbf{k}}(k)$ dominates, these effects can be very dramatic.

Consider now the full three-wave augmented $\widetilde{W}_{00,\mathbf{k}(-\mathbf{k})}$ vs $\sin^2\theta_k$ profiles in graph (b). One can see that the three-wave

term has a major effect on these profiles, especially for low frequencies. This is because the $T_{00,\mathbf{k}(-\mathbf{k})}$ coupling coefficient in Eq. (79) scales with $1/\omega_0$. One can expect, therefore, a significant change in the critical modes at low frequencies due to (1) the more complicated $\widetilde{W}(\theta_k)$ profiles shown in Fig. 3(b), and (2) the effect of a $\mathbf{k}$-dependent relaxation rate on the ultimate critical modes that come out of the analysis. As one example, consider the steeper and steeper fall-off in $\widetilde{W}_{00,\mathbf{k}(-\mathbf{k})}$ with $\sin^2 \theta_k$ at θ_k values close to zero as ω_0/ω_M drops below unity. The effect of this steep fall-off will be to lock the critical modes in to propagation angles very close to $\theta_k = 0$, even as a linear $\eta_{\mathbf{k}}(k)$ function, for example, tries to push the critical mode to higher θ_k values. Keep in mind that these strong effects take place even though three-wave scattering is forbidden.

In the high-frequency limit, the three-wave terms have a vanishing effect on the overall coupling. This accounts for the success of the Suhl or Schlömann theory for the analysis of high power microwave ferrite phenomena for nominal frequencies above 5 GHz or so.

In closing this section, it is useful to add several remarks about spin-wave degeneracy and the $\omega_{\mathbf{k}} = \omega_0$ condition that provides the underpinnings for all of the $(0,0) \rightarrow (\mathbf{k}, -\mathbf{k})$ four-wave process development above. The key point is that there can be situations for which the $\omega_{\mathbf{k}} = \omega_0$ degeneracy constraint disallows some range of spin-wave propagation angles. In the case of bulk spin waves and ellipsoidal samples in the $\omega_0 \gg \omega_M$ high-frequency limit, for example, the degeneracy condition limits the allowed modes to a cone of propagation angles with $\theta_k \le \sin^{-1}(2N_\perp)^{1/2}$. Taken to the extreme $N_\perp \rightarrow 0$ thin film limit, there are no allowed $\mathbf{k}$ modes except at $\theta_k = 0$ and $k = 0$. This corresponds moreover to the well-known FMR situation for perpendicularly magnetized thin films in which the ω_0 operating point sits at the bottom of the band in the $k \rightarrow 0$ limit.

B. Nonlinear spin-wave frequency shift for in-plane magnetized thin films—wave-vector dependence

If one drives the ferromagnetic resonance response or other specific $\mathbf{k} \neq 0$ spin-wave mode to large amplitude, the response is generally accompanied by a shift in the mode frequency. This leads, for example, to well-known effect of classical FMR foldover.[79,80] As noted in the introduction to Sec. VII, these shifts are also central to many nonlinear magnetodynamics problems of current interest. This section is concerned with this nonlinear shift effect.

The discussion starts with a general introduction to the mode shift effect in terms of the Hamiltonian formalism. This is followed by two specific thin-film examples, one for the $\mathbf{k}$-dependent nonlinear frequency shift for an in-plane magnetized film and one for the nonlinear FMR response. The first example, in itself, gives some different insights into nonlinear spin-wave physics in films. The second example, among other things, provides for a direct comparison with exact numerical solutions to the problem and makes for a useful check on the overall formalism. In order to work with tractable equations, these examples are developed in the ultrathin-film limit, for which the dynamic magnetization is

uniform across the film thickness. This corresponds to the type of spin-wave analysis first developed by Harte in 1968[81] and often termed as "the Harte approximation."

The starting point for this discussion is with the general amplitude-driven spin-wave frequency shift. Here, "amplitude" is a loose term. The frequency of a particular spin-wave mode actually depends on the mode amplitude, not in a simple classical sense, but due to the many-fold nonlinear interactions inside the spin-wave system. In principle, many spin-wave modes may be involved in these interactions and the theoretical treatment of this general problem is extremely difficult. A narrower focus is needed for a cogent treatment of the problem. For FMR foldover, soliton dynamics, spin momentum transfer dynamics, and many other of the problems of current interest, one can limit considerations to the self-interaction of a single spin-wave mode only. This is the approach taken here. One first writes the nonlinear spin-wave frequency $\widetilde{\omega}_{\mathbf{k}}$, taken to lowest order in the spin-wave amplitude, as

$$\widetilde{\omega}_{\mathbf{k}} = \omega_{\mathbf{k}} + N|\psi|^2, \tag{80}$$

where $\omega_{\mathbf{k}}$ is the linear spin-wave frequency, developed in Sec. V, N is a nonlinear spin-wave frequency-shift coefficient, and $|\psi|^2$ is a scalar variable that is related in some way to the spin-wave amplitude for the $\mathbf{k}^{\text{th}}$ mode only. The absolute square form is used to emphasize that this scalar variable is real and positive. The crux of the problem is twofold, (1) a proper definition of the spin-wave amplitude parameter $|\psi|^2$ and (2) a self-consistent definition of the nonlinear coefficient N. From the form of Eq. (80), it is clear that the N coefficient alone can have no practical meaning unless it is accompanied by a clearly defined $|\psi|^2$ parameter. The lack of appreciation of this point is perhaps one of the main sources of misinterpretation of many published results in the archival literature. Keep in mind that this newly introduced nonlinear frequency-shift coefficient N is separate and distinct from the previously defined spin-wave tensor $\mathbf{N}_{\mathbf{k}}$ and its components.

Within the framework of the Hamiltonian formalism developed above, $\widetilde{\omega}_{\mathbf{k}}$ can be obtained in a straightforward way. As discussed in Sec. VI, the focus here is on the special case of nonresonant three-wave processes. For this situation, the self-interaction Hamiltonian, $\mathcal{U}_{\text{self}}$, takes the form

$$\mathcal{U}_{\text{self}} \approx \sum_{\mathbf{k}} \omega_{\mathbf{k}} c_{\mathbf{k}}^*(t) c_{\mathbf{k}}(t) + \frac{1}{2} \sum_{\mathbf{k}} \widetilde{W}_{\mathbf{kk},\mathbf{kk}} c_{\mathbf{k}}(t) c_{\mathbf{k}}(t) c_{\mathbf{k}}^*(t) c_{\mathbf{k}}^*(t). \tag{81}$$

This expression follows directly from Eq. (67) with all the subscripted $\mathbf{k}$ values set equal to a single $\mathbf{k}$. The form of Eq. (81) makes clear the formal nature of the self-interaction process. Based on the Hamiltonian of Eq. (81), the equation of motion for a given spin-wave amplitude $c_{\mathbf{k}}(t)$ then takes form

$$i\frac{dc_{\mathbf{k}}(t)}{dt} = \frac{\partial \mathcal{U}_{\text{self}}}{\partial c_{\mathbf{k}}^*(t)} \approx [\omega_{\mathbf{k}} + \widetilde{W}_{\mathbf{kk},\mathbf{kk}}|c_{\mathbf{k}}(t)|^2] c_{\mathbf{k}}(t). \tag{82}$$

One can see immediately that the Eq. (82) describes a simple nonlinear harmonic oscillator with a nonlinear frequency given as

$$\widetilde{\omega}_{\mathbf{k}} = \omega_{\mathbf{k}} + \widetilde{W}_{\mathbf{kk,kk}}|c_{\mathbf{k}}(t)|^2. \tag{83}$$

One can see that Eq. (83) gives precisely the desired result, namely, a consistent and clearly defined nonlinear frequency-shift expression based on physics, not phenomenology. The spin-wave amplitude parameter $|\psi|^2$ is now the square of the modulus of the normal mode $c_{\mathbf{k}}$ spin-wave amplitude. The nonlinear frequency-shift parameter N is just the appropriate four-wave Hamiltonian coefficient with the appropriate three-wave correction, namely, $\widetilde{W}_{\mathbf{kk,kk}}$. This overall result is a natural one, especially if one takes note of the fact that $|c_{\mathbf{k}}|^2$ is a classical analog to the magnon occupation number.

The explicit form of the $\widetilde{W}_{\mathbf{kk,kk}}$ coefficient can be obtained in the same way as for $\widetilde{W}_{00,\mathbf{k}(-\mathbf{k})}$ in Sec. VII A. In the first step, one writes

$$\widetilde{W}_{\mathbf{kk,kk}} = W_{\mathbf{kk,kk}} + T_{\mathbf{kk,kk}}. \tag{84}$$

The bare $W_{\mathbf{kk,kk}}$ four-wave coefficient and the supplemental $T_{\mathbf{kk,kk}}$ three-wave term can be obtained from the general expressions given in Eqs. (63) and (70), respectively. With all the connections between various terms in the $W_{\mathbf{kk,kk}}$ and the $\mathbf{N_k}$ spin-wave tensor components folded in to the analysis, one obtains

$$W_{\mathbf{kk,kk}} = \frac{1}{2}\left[\frac{2\omega_H + \omega_M(N_{xx,\mathbf{k}} + N_{yy,\mathbf{k}})}{2\omega_{\mathbf{k}}}\right]^2$$
$$\times [3\omega_H + \omega_M(2N_{zz,0} + N_{zz,2\mathbf{k}})]$$
$$- \frac{1}{2}[3\omega_H + \omega_M(N_{xx,\mathbf{k}} + N_{yy,\mathbf{k}} + N_{zz,2\mathbf{k}})]. \tag{85}$$

Recall that the ω_H frequency parameter expresses internal static field in the frequency units according to Eq. (46). In a similar way, the $T_{\mathbf{kk,kk}}$ coefficient follows directly from Eq. (70) with $\mathbf{k}_1 = \mathbf{k}_2 = \mathbf{k}_3 = \mathbf{k}_4 = \mathbf{k}$.

$$T_{\mathbf{kk,kk}} = -2\left[\frac{|U_{\mathbf{kk}(2\mathbf{k})}|^2}{\omega_{2\mathbf{k}} + 2\omega_{\mathbf{k}}} + \frac{|V_{\mathbf{kk},(2\mathbf{k})}|^2}{\omega_{2\mathbf{k}} - 2\omega_{\mathbf{k}}} + 4\frac{|V_{\mathbf{k}0,\mathbf{k}}|^2}{\omega_0}\right]. \tag{86}$$

The U and V coefficients can be obtained directly from Eqs. (60) and (61), respectively. For the sake of brevity, it is useful to keep the result for $T_{\mathbf{kk,kk}}$ in general form with no $\mathbf{N_k}$ spin-wave tensor components folded in. Development of the explicit $\mathbf{N_k}$ form leads to a rather complicated and tedious expression with little additional physical content.

It is useful to keep in mind that the above nonlinear frequency-shift equations are in general form and can be applied to any sort of sample with ellipsoidal shape or uniaxial anisotropy, for example, as long as the plane-wave form for the dynamic magnetization self-fields embodied in Eq. (26) applies. In the rest of this section, these expressions will be used for a specific case of a thin isotropic magnetic film with a static field applied at some general angle with respect to the film normal. This basic example is important for many problems of current interest in nonlinear magnetodynamics such as spin momentum transfer and soliton dynamics, to name two examples.

Some remarks are in order before specific results are developed for thin films. First, it is important to note that for isotropic ellipsoidal samples saturated along a principal axis, the $T_{\mathbf{kk,kk}}$ three-wave correction term will vanish in the propagation limits with $\mathbf{k}$ either parallel or perpendicular to the vector static magnetization. This result tracks back to the spin-wave propagation angle dependence of the U and V coefficients in Eq. (86) and to the $N_{xz,\mathbf{k}}$ and $N_{yz,\mathbf{k}}$ parameters in the $D_{\mathbf{k}}$ expression in Eq. (31). It turns out that these terms all vanish in these parallel and perpendicular propagation limits. Perhaps more importantly, note that the second square bracket expression in Eq. (86) contains a $(\omega_{2\mathbf{k}} - 2\omega_{\mathbf{k}})$ denominator term. Keep in mind that this entire analysis is based on the assumption that resonant three-wave processes are not allowed and, more specifically, $(\omega_{2\mathbf{k}} - 2\omega_{\mathbf{k}})$ is never zero. It turns out that for some sample geometries and some specific propagation directions and specific k values, $(\mathbf{k}, \mathbf{k}) \rightarrow 2\mathbf{k}$ three-wave processes may come into resonance. Both of these effects will become evident from the thin-film example developed below.

Turn now to the thin-film analysis in the Harte approximation, that is, in the limit of a very thin film for which the variation in the dynamic magnetization across the film thickness can be neglected. In this limit, any general spin-wave wave vector $\mathbf{k}$ is now constrained to lay in the film plane.[81] The full nonlinear analysis for film parameters outside of the Harte limit is much more complicated. Here, one must deal with a dynamic magnetization and associated fields that vary across the film thickness, the normal magnetostatic modes that come out of the full analysis, and so on. The work of Livesey et al.,[55] noted above, used this more general approach but only for the specific case of an in-plane magnetized film with an in-plane uniaxial anisotropy and for $\mathbf{k}$ values along the field direction only. Even in these limits, the analysis is fairly complicated. For the Harte limit considered for this illustration of the theory, the equations simplify greatly and the physics of the results are made clear. Note that in a confined geometry the number of modes that can interact resonantly through three- or four-wave process is generally reduced. This reduction is due to the quantization of the spin-wave dispersion. In the thin-film geometry considered here the confinement in one dimension still allows for these nonlinear processes since the spectrum for the in-plane wave-vector $\mathbf{k}$ is continuous.

Figure 4 shows the sample geometry. The thin isotropic magnetic film has a thickness d. The film is magnetized to saturation by a uniform static external field $\mathbf{H}_e$ that is applied at an angle θ_H relative to the film normal. The static magnetization, taken as uniform over the film and equal to $\mathbf{M}_s$, is pulled out of the film plane and lies at an angle θ_M, as indicated. The XYZ laboratory reference frame is defined so that the Z axis lies along the film normal, and the $\mathbf{H}_e$ and $\mathbf{M}_s$ vectors lie in the XZ plane. The xyz precessional frame is defined so that the z-axis lines along $\mathbf{M}_s$, the y axis lies along Y, and the x axis is rotated out of the film plane and away from X by the same angle θ_M that separates z and Z. The general in-plane wave-vector $\mathbf{k}$ is taken to have a propagation angle θ_k relative to the X axis.

The components of the effective spin-wave tensor $\mathbf{N_k}$ for the Harte limit with a Z-independent magnetization can be
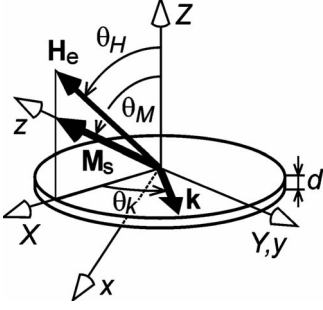
FIG. 4. Isotropic thin-film geometry. One has a *XYZ* laboratory frame coordinate system with *Z* along the film normal and a precession frame *xyz* coordinate system with the *z* along the static equilibrium magnetization direction. The static external field $\mathbf{H_e}$ and the static magnetization vector $\mathbf{M}_s$ are taken to be in the common *XZ* and *xz* planes at angles θ_H and θ_M, respectively, relative to *Z* axis. The general quasi-plane wave spin-wave excitation in the system is taken to have an in-plane wave vector $\mathbf{k}$ at an angle θ_k relative to the *X* direction, as indicated

evaluated relatively easily. The simplest approach is to find the exchange and dipole parts of the spatiotemporal self field $\mathbf{H_M}(\mathbf{r},t)$ from the starting equations in Sec. III, namely, Eqs. (10), (13), and (14). One then uses the Fourier expansion of $\mathbf{H_M}(\mathbf{r},t)$, along with $\mathbf{M}(\mathbf{r},t)=\Sigma_{\mathbf{k}}\mathbf{M_k}(t)e^{i\mathbf{k}\cdot\mathbf{r}}$ to identify the $\mathbf{N_k}$ tensor components defined through Eq. (26). There is one caveat. Even in the case where $\mathbf{M}$ is *Z*-independent, $\mathbf{H_M}$ will still be *Z* dependent. In order to obtain the connection between $\mathbf{M}$ and $\mathbf{H_M}$ in the form of Eq. (26), one first has to average $\mathbf{H_M}(\mathbf{r},t)$ across the film thickness. This step is consistent with the Hamiltonian formulation of the problem. This is due to the fact that the overall approach starts with expressions for the total energy that involves the spatial average of magnetization and all fields over the sample. A more formal and more complicated approach through the use of averaged Green's function, as in Refs. 82 and 83, yields the same exact results. Some straightforward but lengthy algebra yields the isotropic thin-film $\mathbf{N_k}$ tensor components in simple algebraic form.

$$N_{xx,\mathbf{k}} = \alpha_{\mathrm{ex}}k^2 + g_k \cos^2\theta_k \cos^2\theta_M + (1-g_k)\sin^2\theta_M,$$

$$N_{yy,\mathbf{k}} = \alpha_{\mathrm{ex}}k^2 + g_k \sin^2\theta_k,$$

$$N_{zz,\mathbf{k}} = \alpha_{\mathrm{ex}}k^2 + g_k \cos^2\theta_k \sin^2\theta_M + (1-g_k)\cos^2\theta_M,$$

$$N_{xy,\mathbf{k}} = N_{yx,\mathbf{k}} = g_k \sin\theta_k \cos\theta_k \cos\theta_M,$$

$$N_{xz,\mathbf{k}} = N_{zx,\mathbf{k}} = [g_k \cos^2\theta_k - (1-g_k)]\sin\theta_M \cos\theta_M,$$

$$N_{yz,\mathbf{k}} = N_{zy,\mathbf{k}} = g_k \sin\theta_k \cos\theta_k \sin\theta_M. \quad (87)$$

Following Harte, $g_k=1-(1-e^{-kd})/kd$ defines a convenient dipolar thin film function.[81] For a given field angle and $4\pi M_s$ value, the magnetization angle θ_M is an implicit function of H_{e}, θ_H, and $4\pi M_s$, through the static equilibrium condition given in general form in Eq. (42). For the thin-film limit considered here, this condition carries over to a working equation of the form

$$H_{\mathrm{e}}\sin(\theta_M - \theta_H) = 2\pi M_s \sin 2\theta_M. \quad (88)$$

Consider first the linear response and the spin-wave dispersion. From the terms in $\mathbf{N_k}$ listed above, in combination with Eq. (56), one obtains a thin-film spin-wave frequency given by

$$\omega_{\mathbf{k}} = \sqrt{(\omega_H + \omega_M\alpha_{\mathrm{ex}}k^2)(\omega_H + \omega_M\alpha_{\mathrm{ex}}k^2 + \omega_M F_{\mathbf{k}})}. \quad (89)$$

The ω_H frequency factor may be written as

$$\omega_H = |\gamma|H_{\mathrm{e}}\cos(\theta_M - \theta_H) - \omega_M \cos^2\theta_M. \quad (90)$$

The $F_{\mathbf{k}}$ function can be written in the form

$$F_{\mathbf{k}} = g_k + \sin^2\theta_M\left[1 - g_k(1+\cos^2\theta_k)\right.$$

$$\left. + \frac{\omega_M g_k(1-g_k)\sin^2\theta_k}{\omega_H + \omega_M\alpha_{\mathrm{ex}}k^2}\right]. \quad (91)$$

As a check, one can note that above $\omega_{\mathbf{k}}$ result matches the general Green's function-based thin-film spin-wave dispersion result in Ref. 84 for arbitrary film thickness in the limit of a *z*-independent magnetization. The standard uniform mode FMR frequency for an isotropic thin film of infinite extent, namely,

$$\omega_0 = \sqrt{\omega_H(\omega_H + \omega_M \sin^2\theta_M)} \quad (92)$$

also follows in the $\mathbf{k}=0$ limit.

Turn now to the thin-film $\widetilde{W}_{\mathbf{kk,kk}}$ nonlinear frequency-shift parameter. This parameter can be evaluated in a straightforward way from Eqs. (84)–(92). Note that the uniform-mode FMR frequency ω_0 as well as the spin-wave frequency $\omega_{\mathbf{k}}$ plays a role in the general $\widetilde{W}_{\mathbf{kk,kk}}$ for nonzero $\mathbf{k}$. Even in the very thin-film limiting case considered here, the $\widetilde{W}_{\mathbf{kk,kk}}$ for an arbitrary in-plane $\mathbf{k}$ vector is quite complicated, and a general listing of formulas would serves no overall purpose here. For purposes of discussion, selected results as noted above are given in graphical form. For the second example, namely, the nonlinear uniform-mode thin-film response, some basic working equations are also given.

The specific in-plane film analysis for the first example is for $\theta_H=\theta_M=90°$ and a general in-plane wave-vector $\mathbf{k}$. Figure 5 shows results for $\widetilde{W}_{\mathbf{kk,kk}}$ as a function of wave-number film-thickness kd product for the two limiting case propagation directions with $\mathbf{k}$ oriented parallel ($\theta_k=0$) and perpendicular ($\theta_k=90°$) to the in-plane static field, as indicated. The control parameter here is the film thickness. Figure 6 then shows the $\widetilde{W}_{\mathbf{kk,kk}}$ and $W_{\mathbf{kk,kk}}$ vs. kd response as a function of θ_k. Keep in mind that the $T_{\mathbf{kk,kk}}$ three-wave term vanishes in the $\theta_k=0$ and $\theta_k=90°$ limits. This means that the curves in Fig. 5 show no three-wave effects and the responses are determined by the bare $W_{\mathbf{kk,kk}}$ coefficient only. The $\widetilde{W}_{\mathbf{kk,kk}}$ notation is retained for consistency. The curves for the intermediate angles in Fig. 6 show explicitly the additional effect of the three-wave $T_{\mathbf{kk,kk}}$ term in $\widetilde{W}_{\mathbf{kk,kk}}$. Note that in the linear problem, plots of spin-wave mode frequencies as a function of kd show a universal response for $kd\ll1$ but manifest different dependences on thickness as kd approaches and ex-
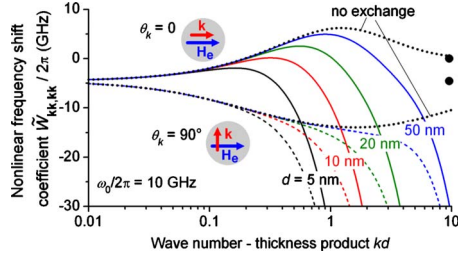
FIG. 5. (Color online) The augmented $\widetilde{W}_{\mathbf{kk},\mathbf{kk}}$ nonlinear frequency-shift coefficient for an in-plane magnetized thin film as a function of the wave number—film thickness kd product for the two limiting case propagation directions with **k** oriented parallel (θ_k =0) and perpendicular (θ_k=90°) to the in-plane static field and for different film thickness d, as indicated. The static field value corresponds to a linear uniform-mode frequency of 10 GHz. The curves labeled "no exchange" show results without exchange. The two dots on the right-hand edge represent the limit values of the no exchange curves for $kd \gg 1$.

ceeds unity. The nonlinear frequency-shift responses show similar effects.

Consider first the $\widetilde{W}_{\mathbf{kk},\mathbf{kk}}$ vs kd plots in Fig. 5. These plots were calculated for different film thicknesses (d), as indicated. The various curves show results for **k** vectors parallel (θ_k=0) and perpendicular (θ_k=90°) to the in-plane static field $\mathbf{H}_e$, as indicated by the inset diagrams. The solid and dashed curve calculations were done for $|\gamma|/2\pi$ =2.8 MHz/Oe, $4\pi M_s$=10 kG, $A=1.1\times10^{-6}$ erg/cm, and H_e=1.114 kOe. These are typical parameter values for permalloy. The selected H_e value corresponds to a small signal limit FMR frequency of 10 GHz. The dotted curves are in the nonexchange limit with $A=0$.

The $\widetilde{W}_{\mathbf{kk},\mathbf{kk}}(kd)$ plots in Fig. 5 show the somewhat complicated nature of the nonlinear response, even for this special case. From the two dotted curves for $A=0$, one can see that there are common profiles that scale with the kd product, with no change in the response for different thicknesses. For $kd \ll 1$ the $\widetilde{W}_{\mathbf{kk},\mathbf{kk}}$ values are negative and converge to a common value in the $kd \to 0$ limit. As kd increases, the θ_k=0 and θ_k=90° curves for $A=0$ split for kd values in the range of
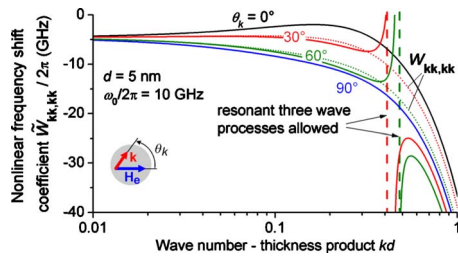

FIG. 6. (Color online) The augmented $\widetilde{W}_{\mathbf{kk},\mathbf{kk}}$ (solid lines) and bare $W_{\mathbf{kk},\mathbf{kk}}$ (dotted lines) nonlinear frequency-shift coefficients for an in-plane magnetized thin film as a function of the wave number—film thickness kd product. Curves are shown for different propagation angles θ_k, as indicated. The static field value corresponds to the linear uniform-mode frequency of 10 GHz. The film thickness is 5 nm. The vertical dashed lines denote kd values at which the resonant three-wave processes are allowed

0.1–1 and then appear to turn over. In the $kd \gg 1$ limit, these curves converge to values indicated by the solid dots shown between the dotted curves at the right-side edge of the plot. The inclusion of exchange changes the profiles completely. With exchange included, curves for the different thickness films split off from the common $A=0$ one by one by one as d is increased. All of the $A \neq 0$ curves show abrupt downward shifts for large kd values. Had these curves been plotted versus k rather than kd, the whole ensemble of curves would show a different perspective. The exchange free curves for the different thicknesses would not show a common response but would shift to higher and higher k values as the thickness is decreased. This, combined with the split-off effect that moves to the right as d increases, would make for a very nonintuitive display.

One can make a qualitative connection between the $\widetilde{W}_{\mathbf{kk},\mathbf{kk}}(kd)$ plots in Fig. 5 and the nonlinear magnetization response based on the simple heuristic approach already noted above. Recall that in this approach, the frequency-shift coefficient is obtained from the change in the spin-wave frequency if the M_s parameter in the linear dispersion equations is replaced by the static magnetization component along the internal field, taken here as M_z^s. From simple geometric considerations one can see that any increase in the $M_{x,y}$ transverse dynamic magnetization components is accompanied by a decrease in M_z^s. With the decrease in M_z^s from M_s expressed in some appropriate way in terms of $M_{x,y}$, one can obtain some frequency-shift parameter that is qualitatively akin to $\widetilde{W}_{\mathbf{kk},\mathbf{kk}}$.

In the spirit of the above, the fact that the $\widetilde{W}_{\mathbf{kk},\mathbf{kk}}$ for the present example is negative in the $kd \to 0$ limit follows from the relatively simple expression for the uniform-mode frequency expression from Eq. (92) in the $\theta_H = \theta_M = 90°$ limit for in-plane magnetized films. The $M_s \to M_z^s$ replacement in Eq. (92) yields a nonlinear uniform-mode frequency $\widetilde{\omega}_0$ given by $|\gamma|\sqrt{H_e(H_e+4\pi M_z^s)}$. From this, one can see immediately that as the transverse dynamic magnetization increases and M_z^s decreases, $\widetilde{\omega}_0$ will also decrease. This gives a negative frequency-shift coefficient that is consistent with the negative value of $\widetilde{W}_{\mathbf{kk},\mathbf{kk}}$ at $kd \ll 1$ in Fig. 5.

The heuristic approach also provides some qualitative understanding for intermediate kd values. As the kd increases, the splitting in the $\widetilde{W}_{\mathbf{kk},\mathbf{kk}}$ response with an increase for θ_k =0 (upper curves) and a decrease for θ_k=90° (lower curves) is due to dipolar effects. The linear $\omega_{\mathbf{k}}(k)$ response for θ_k =0 corresponds to the well-known Damon-Eshbach (DE) magnetostatic backward volume wave (MSBVW) dispersion. For MSBVW excitations, $\omega_{\mathbf{k}}(k)$ drops down from the uniform-mode frequency as k increases. For a larger and larger transverse dynamic magnetization and a decreasing M_z^s, there will be less of a drop and the net effect is nonlinear frequency coefficient shifted toward positive values. The situation is reversed for θ_k=90°. Here, one is dealing with the DE magnetostatic surface wave excitations. For these, the linear $\omega_{\mathbf{k}}(k)$ increases with as k increases. As above, this dipole effect is reduced as M_z^s and the nonlinear frequency response coefficient decreases.

In the short wavelength high kd limit the response is dominated by exchange interactions. In this case, the $\omega_{\mathbf{k}}$

spin-wave frequency can be approximated as $\omega_k \approx |\gamma|(H_e + 4\pi M_z^s \alpha_{ex} k^2)$. Based on the above described heuristic analysis, one can see immediately that in this case ω_k decreases in proportion to k^2. This is the origin of the rapid downturn in $\widetilde{W}_{\mathbf{kk,kk}}$ vs kd curves in Fig. 5 at large kd.

Turn now to the results as a function of propagation angle in Fig. 6 and the specific effect of three-wave processes on the nonlinear frequency-shift coefficient vs kd response. In order to make these effects explicit, curves for both the full $\widetilde{W}_{\mathbf{kk,kk}}$ (solid lines) and the bare $W_{\mathbf{kk,kk}}$ (dotted lines) coefficients are shown. The plots were calculated for a film thickness of 5 nm and different θ_k propagation angles, as indicated. The inset provides a reminder of the propagation geometry. The calculations were done for the same material parameters as those shown in Fig. 5. As noted above, the three-wave $T_{\mathbf{kk,kk}}$ term vanishes for $\theta_k = 0$ and $\theta_k = 90°$ so that in these limits the $\widetilde{W}_{\mathbf{kk,kk}}$ and $W_{\mathbf{kk,kk}}$ coefficients are the same. The vertical dashed lines denote the kd values at which the $\widetilde{W}_{\mathbf{kk,kk}}$ vs kd responses diverge for intermediate propagation angles. This divergence effect will be discussed shortly.

Consider first the end limit $\widetilde{W}_{\mathbf{kk,kk}}$ and the bare $W_{\mathbf{kk,kk}}$ vs kd curves for the intermediate angles. One can see that nonlinear shift vs kd responses change gradually and continually as one moves from one end-limit propagation angle to the other. When, however, the effects of the three-wave $T_{\mathbf{kk,kk}}$ terms are included, as with the intermediate solid-line $\widetilde{W}_{\mathbf{kk,kk}}$ curves, the response changes dramatically. The main effect is in the dramatic divergences in the $\widetilde{W}_{\mathbf{kk,kk}}$ vs kd profiles noted above. This divergence is a consequence of the resonant three-wave processes that take place at particular $\mathbf{k}$ wave vectors that are defined by the (kd, θ_k) combinations indicated from the curves. At these specific points, three-wave process of the form $(\mathbf{k}, \mathbf{k}) \rightarrow 2\mathbf{k}$ become resonant and the $(\omega_{2\mathbf{k}} - 2\omega_{\mathbf{k}})$ denominator term in the $T_{\mathbf{kk,kk}}$ coefficient in Eq. (86) goes to 0. Divergence effect shows, rather dramatically, that one cannot leave out the $\mathcal{U}^{(3)}$ three-wave process terms in the Hamiltonian for spin-wave modes with $\mathbf{k}$ values near these resonant points.

A brief remark about the accuracy of plots in Fig. 5 and 6 is in order here. Keep in mind that these curves were calculated in the Harte approximation with the dynamic magnetization taken as uniform across the film thickness. This approximation has certain limitations. The nonexchange curves in Fig. 5 can be considered approximately correct up to $kd \sim 1$ or so. This is especially critical for θ_k close to 90°. For these angles and for $kd > 1$ the dynamic magnetization across the film thickness has a nonuniform surfacelike character,[85] and the Harte approximation is not valid. However, once the exchange interaction is included, the dynamic magnetization profile becomes nearly constant even for relatively large kd values. The nonlinear coefficient curves in Fig. 5 and 6 with exchange included are therefore valid to a very good approximation over the range of kd values shown.

C. Nonlinear spin-wave frequency shift for the uniform ferromagnetic resonance mode in thin films

Even these relatively simple examples for an in-plane magnetized film shows the complexity of the $\widetilde{W}_{\mathbf{kk,kk}}$ re-

sponses for a general wave vector. Keep in mind that the results shown above were also for a specific set of material parameters, field values, and film thicknesses. In order to provide better overall insight into the nonlinear properties, a second example is included here. This example considers the $\widetilde{W}_{\mathbf{kk,kk}}$ coefficient response in an even more simplified case for the $\mathbf{k} = 0$ limit only. As noted above, this uniform-mode nonlinear frequency-shift coefficient, $\widetilde{W}_{00,00}$, has applications in nonlinear spin-wave dynamics phenomena that include microwave magnetic envelope solitons and spin torque oscillators, for example. For this example, the $\widetilde{W}_{00,00}$ coefficient will denoted simply as a nonlinear coefficient N, in accord with Eq. (80). This is the standard nomenclature used in the literature.

Consider first two special cases, the perpendicular-to-plane (PTP) configuration with $\theta_H = \theta_M = 0$, and the IP configuration with $\theta_H = \theta_M = 90°$. These are most common experimental configurations that have been treated theoretically in numerous previous works. One can evaluate the N, that is, $\widetilde{W}_{00,00}$, coefficient from the general response equations given in Eqs. (84)–(86). For the PTP configuration, one has

$$N_{\mathrm{PTP}} = \omega_M. \tag{93}$$

For the IP configuration one obtains

$$N_{\mathrm{IP}} = -\frac{\omega_M}{8\omega_0^2}(4\omega_H + \omega_M) \tag{94}$$

with $\omega_H = |\gamma| H_e$ and $\omega_0 = \sqrt{\omega_H(\omega_H + \omega_M)}$.

The N_{PTP} coefficient in Eq. (93) corresponds to the well-known result reported in several places.[69,71,72] The N_{IP} in the form given in Eq. (94), however, has not been reported previously. As already indicated, however, one must be cautious in the detailed comparison of different results because any specific nonlinear frequency-shift parameter will be tied closely to the exact definition of the amplitude parameter $|\psi|^2$.

Table I present a tabulation of selected working expressions that provide a means of comparison between previous results and those from this work. Table I is limited to results for the in-plane magnetized film nonlinear frequency-shift coefficient N_{IP}. Rows A, B, and C list previously reported results. Row D corresponds to the result from Eq. (94). Along with each listed N_{IP} coefficient, the applicable definition of the dynamic magnetization amplitude parameter $|\psi|^2$ is also given. The listed $|\psi|^2$ expressions are all cast in terms of parameters and notation used in this work.

Details on the analyses that give the expressions in A, B, and C can be found in the cited references. The approaches that lead to the N_{IP} expressions in A and B come from simple heuristic considerations of the reduction in the longitudinal static component of magnetization from the saturation magnetization M_s. Operationally, these frequency-shift expressions are obtained though the substitution of the effective amplitude reduced "static" magnetization in the z direction for M_s in the spin-wave frequency expressions from the linear theory. The difference between A and B approaches is in the definition of the amplitude parameter and in the treatment

TABLE I. Summary of expressions from this and various other works for the uniform ferromagnetic resonance-mode nonlinear frequency-shift parameter N_{IP} for an in-plane magnetized thin film.

Approach	Frequency-shift parameter N_{IP}	Approach-specific amplitude parameter $|\psi|^2$	Reference
A	$N_{IP} = -\frac{\omega_M \omega_H}{2\omega_0}$	$1 - M_z^s/M_s$	Ref. 86, Eq. 15
B	$N_{IP} = -\frac{\omega_M \omega_H}{4\omega_0}\left(1 + \frac{\omega_H^2}{\omega_0^2}\right)$	$(M_{y\,max}/M_s)^2/2$	Ref. 69, Eq. 18
C	$N_{IP} = -\frac{\omega_H \omega_M}{\omega_0}\frac{\omega_H + \omega_M/4}{\omega_H + \omega_M/2}$	$\frac{\omega_H + \omega_M/2}{2\omega_0}|c_0|^2$	Ref. 75, Eq. (3.29a)
D	$N_{IP} = -\frac{\omega_M \omega_H}{8\omega_0^2}(4\omega_H + \omega_M)$	$|c_0|^2$	This work, Eq. (94)

of the magnetization precession ellipticity. For A approach, the amplitude parameter $|\psi|^2$ is defined through the M_z^s static magnetization component along the internal field, and the effect of the ellipticity of the spin precession, in a classical view, is not taken into account. For B, the $|\psi|^2$ is defined through the amplitude of in-plane dynamic magnetization component, taken here as $M_{y\,max}$, and the ellipticity is thereby included explicitly.

The result in C is from a nonlinear analysis by Slavin and Tiberkevich done in a similar way to the present work with summary results only given in Ref. 74. One can easily check that the expressions in C match the results in D from this work.

The accuracy of the various expressions in Table I can be compared with exact results obtained from through direct numerical integration of the torque equation of motion for the dynamic magnetization in Eq. (1). It is noteworthy that such a comparison has never been provided, as far as authors know. Details on the numerical procedure are given in the Appendix. In brief, one numerically calculates the magnetization free-precession traces for different initial amplitudes. From these traces one obtains the frequency of the precession, $\tilde{\omega}_0$. The traces can also be used to extract appropriate $|\psi|^2$ amplitude parameters from the definitions in Table I and the expressions developed in earlier sections that connect c_0 to the actual magnetization dynamics. From the initial slope of the $\tilde{\omega}_0$ vs $|\psi|^2$ response, one then gets the nonlinear frequency-shift coefficient N_{IP}.

Figure 7 shows the results of these comparisons. The symbols show the N_{IP} data obtained numerically. The lines show computed curves from the expressions in Table I. The labels for each pair of numerical and theoretical results match the nomenclature of Table I. The calculations were done for $|\gamma|/2\pi = 2.8$ MHz/Oe, $4\pi M_s = 10$ kG, and a static field range that corresponds to linear frequency $\omega_0/2\pi$ values from 1 to 100 GHz. Note that both axes are shown on a logarithmic scale and that all N_{IP} values are negative. The negative frequency shifts are the physical consequence of the basic FMR condition for an in-plane magnetized film, $\omega_0 = \sqrt{\omega_H(\omega_H + \omega_M)}$. Any increase in amplitude by whatever model one chooses results in a decrease in M_z^s from M_s, a corresponding drop in the effective value of ω_M, and a *decrease* in the FMR frequency. Note also that the apparent differences between the actual N_{IP} values obtained from the different working equations are due to the different definitions of the amplitude parameter. The only meaningful quantitative comparisons are for the *pairs* of analytical solid

curve and numerical point-by-point results for a single model. That is the pairs of results indicated for A, B, C, and D.

Consider first the A and B results. One can clearly see that these analytical heuristic approaches, based only on the dynamic reduction in M_z^s from M_s, do not give a good match to the exact numerical results except in the extreme high-frequency and high-field limits. In the low-frequency limit, moreover, the discrepancies between the exact numerical results and the analytical expressions are on the order of a factor of 2. The fact that the discrepancy becomes smaller as the frequency increases will be discussed shortly. In contrast, the analytical results for C and D, as obtained from the full nonlinear theory, can be seen to give a nearly perfect match to the numerical results. This agreement provides a check that the full nonlinear analysis formalism developed in this work, albeit rather involved and algebraically complex, is (1) correct and (2) comprises a valid approach for the analysis of nonlinear spin-wave dynamics.

The inaccuracy of the heuristic approaches under A and B comes from the fact that they both start from a purely linear analysis with the nonlinearity folded in only through the reduction of the static component of the magnetization. This approach cannot therefore, in principle, catch all complex details of the nonlinear dynamics. The only case when the heuristic approach gives the correct answer is in the circular magnetization precession limit. This is the reason why the accuracy of A and B results in Fig. 7 improves for high frequencies. For these frequencies, where the static field is large, the precession is closer and close to a purely circular
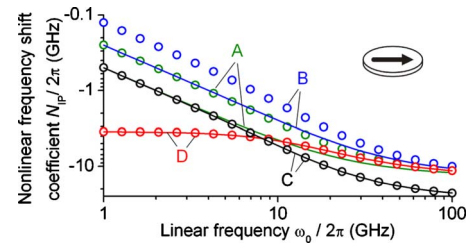

FIG. 7. (Color online) Uniform-mode nonlinear frequency-shift parameter N_{IP} for an in-plane magnetized thin film as a function of the linear uniform mode frequency ω_0. The symbols denote exact values obtained from numerical integration of magnetization torque equation. The solid curves show analytical results based on the expressions in Table I. The A, B, C, and D labels for each pair of points and curves correspond to the approaches and expressions in the A, B, C, and D rows of Table I, respectively.

polarization response. These approaches also are valid for the PTP magnetization configuration. In this case, $|c_0|^2$ is analytically equal to $1-M_z^s/M_s$. Unfortunately, much of the literature uses this same approach for configurations other than the PTP case. The present results show that this is not correct.

The final item of discussion for this section concerns the uniform-mode nonlinear frequency shift $N(\theta_M)$ for an obliquely magnetized isotropic thin film. This result can be cast into the form

$$N(\theta_M) = \omega_M \frac{\omega_H^2}{8\omega_0^4}[\omega_M(3\omega_H - \omega_M)\sin^4 \theta_M - 4\omega_H(2\omega_M$$
$$+ 3\omega_H)\sin^2 \theta_M + 8\omega_H^2] \qquad (95)$$

with ω_H and ω_0 given in Eq. (90) and (92), respectively. The equilibrium magnetization angle θ_M for a given field angle θ_H is determined from the implicit expression in Eq. (88). Note that for the PTP and IP limits at $\theta_H=\theta_M=0$ and $\theta_H=\theta_M=90°$, respectively, Eq. (95) reduces to appropriate limits already given in Eqs. (93) and (94). The accuracy of the $N(\theta_M)$ expression in Eq. (95) can be easily checked by comparison with exact numerical values, just as before.

Comparisons with the heuristic approach based on the nonlinear magnetization M_z^s reduction effect only can be done in a similar way, based on the published analyses in Refs. 32 and 68, among others. The corresponding heuristic $N(\theta_M)$ result, cast in terms of the parameter definitions in this work and now labeled as $N_{\text{heu}}(\theta_M)$, may be written in the form

$$N_{\text{heu}}(\theta_M) = \frac{\omega_M \omega_H}{2\omega_0} \frac{2 - (1 + \omega_M/\omega_H)\tan^2 \theta_M}{1 + (1 + \omega_M/\omega_H)\tan^2 \theta_M}. \qquad (96)$$

Keep in mind that the companion amplitude parameter for this frequency-shift function is given by $|\psi|^2=1-M_z^s/M_s$, as in line A of Table I.

Figure 8 shows selected analytical and exact numerical results for the nonlinear frequency shift N as a function of magnetization angle θ_M. The symbols in both graphs show values from numerical integration. The corresponding points in the (a) and (b) graphs are a little different because of the different definitions of the $|\psi|^2$ amplitude parameter. The curves in graphs (a) and (b) show the analytical results for $N(\theta_M)$ and $N_{\text{heu}}(\theta_M)$, respectively. The calculations were done for three values of ω_0 The labels in the graphs indicate the applicable values of $\omega_0/2\pi$ for the three selected cases, namely, 1, 5, and 20 GHz. All of the calculations were done for $|\gamma|/2\pi=2.8$ MHz/Oe and $4\pi M_s=10$ kG.

The results in graph (a) confirm, for the general oblique magnetization case that the present analysis provides an accurate representation of the nonlinear FMR response. One can see, however, that the match up in graph (b) between the exact N values and the heuristic analytical response is very poor. This demonstrates, once again, that the simple heuristic approach based on the reduction in M_z^s from M_s does not provide an accurate model of the nonlinear response for magnetization orientations away from the PTP configuration. One can see that all the exact values and curves in both
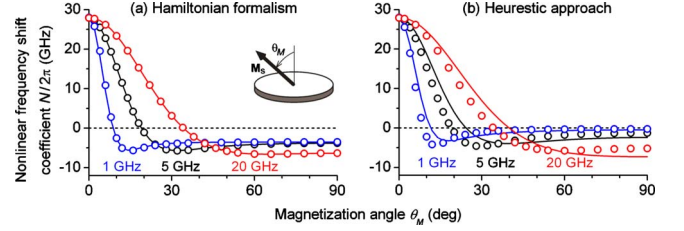

FIG. 8. (Color online) Uniform-mode nonlinear frequency-shift coefficient N as a function of the magnetization angle θ_M with respect to the film normal, as indicated in the inset. The symbols denote results obtained from numerical integration of the magnetization torque equation. The lines show analytical results from the models given in text. The calculations were done for the static field values that correspond to fixed uniform-mode linear frequency ω_0 values, as indicated. Graph (a) shows results based on theory presented in this paper. Graph (b) shows results based on the heuristic nonlinear magnetization M_s^z reduction approach.

graphs converge to a single value at $N/2\pi=\omega_M/2\pi=28$ GHz at $\theta_M=0$. This is consistent with Eq. (93) and the pure circularly polarized nature of the precession in this limit.

Turn now to the actual $N(\theta_M)$ and $N_{\text{heu}}(\theta_M)$ responses in Fig. 8. As the magnetization is gradually tilted from the film normal and θ_M is increased, the N parameter decreases and eventually becomes negative. This is in accord with physical considerations for the IP in-plane configuration discussed earlier. There exists therefore a magnetization angle, taken here as θ_{M0}, at which the nonlinear frequency shift is zero. The θ_{M0} values in this particular example, determined from the numerical data, are 9°, 19°, and 34°, for $\omega_0/2\pi=1$, 5, and 20 GHz, respectively. Note that these θ_{M0} values are the same in both graphs (a) and (b). Since the θ_{M0} corresponds to the situation when the nonlinear frequency does not depend on the magnetization precession magnitude, this value cannot, obviously, depend on the definition of the amplitude parameter.

The results in Fig. 8(a) again confirm that the analytical result obtained in this work, as given in Eq. (95), match the exact numerical results extremely well over the entire range of magnetization angles. The heuristic result given in Eq. (96) and shown in graph (b), on the other hand, differs noticeably from the exact response. It is also important to note that the nonlinear frequency-shift coefficient N in this work was obtained with the explicit inclusion of the three-wave correction term in $T_{00,00}$. This inclusion is critical. Without this term, that is, with only the bare four-wave term $N=W_{00,00}$ taken alone, the shift parameter N is very far from the exact result. This demonstrates again that the full nonlinear analysis is required for the correct description of the nonlinear spin-wave dynamics.

VIII. SUMMARY

A systematic step-by-step development of nonlinear spin-wave theory within the framework of a Hamiltonian formalism has been presented. The Hamiltonian is cast in the form of an expansion with terms up to fourth order in the canoni-

cal spin-wave amplitudes. Analytic expansion coefficients are given in a general form, for a general orientation of the external field relative to the static magnetization direction and a general spin-wave propagation direction. The general working equations should be useful for the theoretical analysis of a wide variety of problems in nonlinear magnetodynamics in saturated magnetic systems.

In order to demonstrate the power of the theory, two specific examples have been provided. The first considers the coupling coefficients for Suhl second-order instability processes for a magnetically saturated sample in the form of an ellipsoid of revolution. It is shown that the inclusion of three-wave correction terms, not considered before, can significantly modify the value of the spin-wave instability threshold. In the second example, nonlinear spin-wave frequency-shift formulae are developed for a thin-film geometry. In particular, it is shown that a strict application of theory yield analytical results for the uniform-mode nonlinear frequency-shift coefficient that are in near perfect agreement with exact results obtained by numerical methods. For completeness, it is also shown that predictions based on simple heuristic considerations of the decrease on the near-static value of the saturation magnetization as the classical precession angle increases gives frequency-shift parameters that can deviate significantly from the exact response.

ACKNOWLEDGMENTS

APPENDIX

This appendix provides details on the determination of the uniform-mode nonlinear frequency-shift coefficient N from the numerical integration of torque equation. As follows from Eq. (80), one has to do two things. (1) One must determine the uniform-mode nonlinear eigenfrequency $\tilde{\omega}_0$ from the numerical solution to torque equation. (2) One must also find the correct amplitude parameter $|\psi|^2$ for comparison of the response with the specific model of interest. The appropriate nonlinear response coefficient N can be then obtained as a slope of the numerically determined $\tilde{\omega}_0$ vs $|\psi|^2$ curve. By definition, the $|\psi|^2=0$ intercept defines the linear limit eigenfrequency ω_0.

The problem geometry has been given in Fig. 1. The effective field for a uniformly magnetized thin film in the laboratory XYZ frame consists of the sum of the vector static external field and static demagnetizing field perpendicular to the film plane. This field can be therefore written as $\mathbf{H}_{\text{eff}}(t) = \mathbf{H}_e - 4\pi M_Z(t)\hat{\mathbf{Z}}$. The numerical integration of the torque equation with an initial condition $\mathbf{M}(t=0)=\mathbf{M}_0$ then yields time dependence of the magnetization vector $\mathbf{M}(t)$ in XYZ frame. With the knowledge of the static magnetization angle θ_M, which can be obtained from the static equilibrium con-

dition, one can find the magnetization components $M_{x,y,z}(t)$ in the precessional xyz frame. Since there is no damping included in the calculation, there is no transient response in the $\mathbf{M}(t)$ dependence and the magnetization vector will undergo a precession motion with an eigenfrequency $\tilde{\omega}_0$ which is, besides other simulation parameters, determined by the precession magnitude. The frequency $\tilde{\omega}_0$ can be then found from the time traces of the transverse components $M_{x,y}(t)$. Note that all calculations presented here were done for precession amplitudes for which the $M_{x,y}(t)$ responses were fairly sinusoidal and with well-defined frequencies.

The amplitude parameter $|\psi|^2$ is found from the dynamic magnetization components $M_{x,y,z}(t)$ in a straightforward way that depends on definition of $|\psi|^2$ for the particular model of interest. Consider, for example, the connection for the current Hamiltonian theory, $|\psi|^2=|c_0|^2$. From Eqs. (4) and (5), one can obtain the complex spin-wave amplitude parameter $a_0(t)$ as

$$a_0(t) = \frac{iM_x(t) + M_y(t)}{\sqrt{M_s + M_z(t)}}. \tag{A1}$$

The circular uniform mode complex amplitude $b_0(t)$ is then given by the inverse transform to Eq. (53). This transformation yields the connection

$$b_0(t) = u_0 a_0(t) - v_0 a_0^*(t). \tag{A2}$$

Here, the u_0 and v_0 coefficients are evaluated in the $\mathbf{k}=0$ limit from Eqs. (54) and (55), respectively. Finally, one obtains $|c_0|^2$ from the solution to the quadratic equation

$$\left(\frac{45|V_{00,0}|^2 + |U_{000}|^2}{9\omega_0^2}\right)(|c_0|^2)^2 + |c_0|^2 - |b_0|^2 = 0. \tag{A3}$$

This working equation follows from Eq. (66) with rapidly oscillating terms such as $c_0^2|c_0|^2$ neglected. As a practical note, the coefficient of the quadratic $|c_0|^4$ term in Eq. (A3) is relatively small. This means that one can also use the approximation $|b_0|^2 \approx |c_0|^2$ with no significant change in the final result.

The numerical procedure to find the uniform-mode nonlinear frequency-shift coefficient N is as follows. Step 1. Nu-
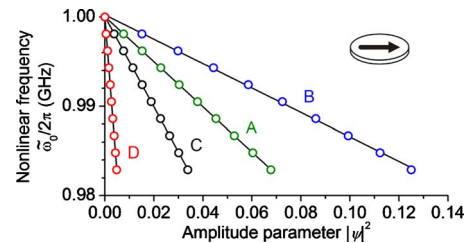

FIG. 9. (Color online) The uniform-mode nonlinear frequency $\tilde{\omega}_0$ as a function of the amplitude parameter $|\psi|^2$ for an in-plane magnetized thin film. The labels correspond to rows A–D in Table I. The symbols denote results from numerical integration of the torque equation of motion for the dynamic magnetization. The solid lines show linear fits to the numerical results. The numerical response was obtained for permalloy parameters. The in-plane static field of 12.7 Oe corresponds to a linear low amplitude limit uniform-mode frequency of 1 GHz.

merically integrate the torque equation of motion for a given set of parameters. Step 2. Use the actual time traces of magnetization vector components in the precessional xyz frame to obtain the uniform-mode precession eigenfrequency $\tilde{\omega}_0$ along with value of the amplitude parameter $|\psi|^2$ for different precession amplitude levels. Step 3. Take the nonlinear frequency-shift coefficient N as the slope of the $\tilde{\omega}_0$ vs $|\psi|^2$ response from the numerical values obtained in (1) and (2).

Figure 9 shows an example of the $\tilde{\omega}_0$ vs $|\psi|^2$ response obtained for a permalloy thin film and the in-plane ($\theta_H = \theta_M = 90°$) field/magnetization configuration. The A through D labels for the four $\tilde{\omega}_0$ vs $|\psi|^2$ responses shown connect the computed responses to the corresponding lines in Table I.

The linear response frequency of 1 GHz in the $|\psi|^2 \rightarrow 0$ limit corresponds to an in-plane static field of 12.7 Oe. The symbols show numerical results obtained from the magnetization time traces as described above. The lines show linear fits to these points. The maximum value of the actual magnetization precessional angle was about 30°.

One can see that nonlinear frequency-shift scales linearly with the FMR amplitude $|\psi|^2$ parameter up to relatively large precession angles. The slope of these responses gives, therefore, valid values of the nonlinear frequency-shift coefficient N for the comparisons with the model calculations discussed in the sections above.

*Present address: University of Colorado at Colorado Springs, Colorado Springs, Colorado 80918.

[1] N. Bloembergen and R. W. Damon, Phys. Rev. **85**, 699 (1952).

[2] R. W. Damon, Rev. Mod. Phys. **25**, 239 (1953).

[3] N. Bloembergen and S. Wang, Phys. Rev. **93**, 72 (1954).

[4] W. Wettling, W. D. Wilber, P. Kabos, and C. E. Patton, Phys. Rev. Lett. **51**, 1680 (1983).

[5] V. V. Naletov, G. de Loubens, V. Charbois, O. Klein, V. S. Tiberkevich, and A. N. Slavin, Phys. Rev. B **75**, 140405 (2007).

[6] T. S. Hartwick, E. R. Peressini, and M. T. Weiss, J. Appl. Phys. **32**, S223 (1961).

[7] G. Gibson and C. Jeffries, Phys. Rev. A **29**, 811 (1984).

[8] F. M. de Aguiar and S. M. Rezende, Phys. Rev. Lett. **56**, 1070 (1986).

[9] B. A. Kalinikos, N. G. Kovshikov, and A. N. Slavin, Sov. Phys. JETP **67**, 303 (1988).

[10] M. Chen, M. A. Tsankov, J. M. Nash, and C. E. Patton, Phys. Rev. Lett. **70**, 1707 (1993).

[11] M. Wu, B. A. Kalinikos, L. D. Carr, and C. E. Patton, Phys. Rev. Lett. **96**, 187202 (2006).

[12] E. B. Myers, D. C. Ralph, J. A. Katine, R. N. Louie, and R. A. Buhrman, Science **285**, 867 (1999).

[13] S. I. Kiselev, J. C. Sankey, I. N. Krivorotov, N. C. Emley, R. J. Schoelkopf, R. A. Buhrman, and D. C. Ralph, Nature (London) **425**, 380 (2003).

[14] Y. M. Yakovlev, Y. N. Burdin, Y. R. Shilnikov, and T. N. Bushueva, Sov. Phys. Solid State **12**, 2475 (1971).

[15] C. E. Patton and W. Jantz, J. Appl. Phys. **50**, 7082 (1979).

[16] A. V. Nazarov, D. Ménard, J. J. Green, and C. E. Patton, J. Appl. Phys. **94**, 7227 (2003).

[17] B. K. Kuanr and A. V. Kuanr, Phys. Status Solidi A **153**, 191 (2006).

[18] G. A. Melkov and S. V. Sholom, Sov. Phys. JETP **96**, 712 (1989).

[19] A. V. Nazarov and C. E. Patton, J. Appl. Phys. **93**, 9195 (2003).

[20] J. B. Comly, T. Penney, and R. V. Jones, J. Appl. Phys. **34**, 1145 (1963).

[21] A. Berteaud and H. Pascard, J. Appl. Phys. **36**, 970 (1965).

[22] Y. Khivintsev, B. Kuanr, T. J. Fal, M. Haftel, R. E. Camley, Z. Celinski, and D. L. Mills, Phys. Rev. B **81**, 054436 (2010).

[23] B. K. Kuanr, Y. V. Khivintsev, A. Hutchison, R. E. Camley, and Z. J. Celinski, IEEE Trans. Magn. **43**, 2645 (2007).

[24] S. Y. An, P. Krivosik, M. A. Kramer, H. M. Olson, A. V. Nazarov, and C. E. Patton, J. Appl. Phys. **96**, 1572 (2004).

[25] H. M. Olson, P. Krivosik, K. Srinivasan, and C. E. Patton, J. Appl. Phys. **102**, 023904 (2007).

[26] T. Gerrits, P. Krivosik, M. L. Schneider, C. E. Patton, and T. J. Silva, Phys. Rev. Lett. **98**, 207602 (2007).

[27] L. Berger, Phys. Rev. B **54**, 9353 (1996).

[28] J. C. Slonczewski, J. Magn. Magn. Mater. **159**, L1 (1996).

[29] J. A. Katine, F. J. Albert, R. A. Buhrman, E. B. Myers, and D. C. Ralph, Phys. Rev. Lett. **84**, 3149 (2000).

[30] W. H. Rippard, M. R. Pufall, S. Kaka, S. E. Russek, and T. J. Silva, Phys. Rev. Lett. **92**, 027201 (2004).

[31] J. C. Sankey, P. M. Braganca, A. G. F. Garcia, I. N. Krivorotov, R. A. Buhrman, and D. C. Ralph, Phys. Rev. Lett. **96**, 227601 (2006).

[32] A. N. Slavin and P. Kabos, IEEE Trans. Magn. **41**, 1264 (2005).

[33] S. M. Rezende, F. M. de Aguiar, and A. Azevedo, Phys. Rev. Lett. **94**, 037202 (2005).

[34] H. Suhl, J. Phys. Chem. Solids **1**, 209 (1957).

[35] E. Schlömann, J. J. Green, and U. Milano, J. Appl. Phys. **31**, S386 (1960).

[36] C. E. Patton, Phys. Status Solidi B **92**, 211 (1979).

[37] A. V. Nazarov, C. E. Patton, R. G. Cox, L. Chen, and P. Kabos, J. Magn. Magn. Mater. **248**, 164 (2002).

[38] L. D. Landau and E. M. Lifshitz, Phys. Z. Sowjetunion **8**, 153 (1935).

[39] E. Schlömann, Technical Report No. R-48, 1959 (unpublished).

[40] E. Schlömann, Phys. Rev. **116**, 828 (1959).

[41] V. S. L'vov, *Wave Turbulence Under Parametric Excitation* (Springer-Verlag, Berlin, 1994).

[42] *Nonlinear Waves and Weak Turbulence*, edited by V. E. Zakharov (American Mathematical Society, Providence, 1998).

[43] V. S. L'vov, Phys. Rep. **207**, 1 (1991).

[44] Yu. Lvov and E. G. Tabak, Physica D **195**, 106 (2004).

[45] G. Falkovich, Phys. Rev. Lett. **69**, 3173 (1992).

[46] E. A. Kuznetsov, J. Exp. Theor. Phys. **93**, 1052 (2001).

[47] F. Sahraoui, G. Belmont, and L. Rezeau, Phys. Plasmas **10**, 1325 (2003).

[48] V. E. Zakharov and S. V. Nazarenko, Physica D **201**, 203 (2005).

[49] V. E. Zakharov, V. S. L'vov, and S. S. Starobinets, Sov. Phys. Solid State **11**, 2368 (1970).

[50] V. E. Zakharov, V. S. L'vov, and S. S. Starobinets, Sov. Phys.

Usp. **17**, 896 (1975).

[51] V. E. Zakharov and V. S. L'vov, Sov. Phys. Solid State **14**, 2513 (1973).

[52] V. E. Zakharov and V. S. L'vov, Radiophys. Quantum Electron. **18**, 1084 (1975).

[53] V. E. Zakharov, V. S. L'vov, and G. Falkovich, *Kolmogorov Spectra of Turbulence I* (Springer-Verlag, Berlin, 1992).

[54] A. Yu. Dobin and R. H. Victora, Phys. Rev. Lett. **90**, 167203 (2003).

[55] K. L. Livesey, M. P. Kostylev, and R. L. Stamps, Phys. Rev. B **75**, 174427 (2007).

[56] J. V. Kim, V. Tiberkevich, and A. N. Slavin, Phys. Rev. Lett. **100**, 017207 (2008).

[57] M. Grimsditch, L. Giovannini, F. Montoncello, F. Nizzoli, G. K. Leaf, and H. G. Kaper, Phys. Rev. B **70**, 054409 (2004).

[58] V. E. Zakharov, Sov. Phys. JETP **24**, 740 (1967).

[59] P. Krivosik, N. Mo, S. Kalarickal, and C. E. Patton, J. Appl. Phys. **101**, 083901 (2007).

[60] T. Holstein and H. Primakoff, Phys. Rev. **58**, 1098 (1940).

[61] J. D. Jackson, *Classical Electrodynamics* (Wiley, New York, 1998).

[62] M. Chen and C. E. Patton, in *Nonlinear Phenomena and Chaos in Magnetic Materials*, edited by P. E. Wigen (World Scientific, Singapore, 1994), Chap. 3.

[63] M. A. Hoefer, T. J. Silva, and M. D. Stiles, Phys. Rev. B **77**, 144401 (2008).

[64] S. M. Rezende, F. M. de Aguiar, and A. Azevedo, Phys. Rev. B **73**, 094402 (2006).

[65] A. N. Slavin, B. A. Kalinikos, and N. G. Kovshikov, in *Nonlinear Phenomena and Chaos in Magnetic Materials*, edited by P. E. Wigen (World Scientific, Singapore, 1994), Chap. 9.

[66] B. Georges, J. Grollier, M. Darques, V. Cros, C. Deranlot, B. Marcilhac, G. Faini, and A. Fert, Phys. Rev. Lett. **101**, 017201 (2008).

[67] V. P. Krasitskii, Sov. Phys. JETP **71**, 921 (1990).

[68] G. Gerhart, E. Bankowski, G. A. Melkov, V. S. Tiberkevich, and A. N. Slavin, Phys. Rev. B **76**, 024437 (2007).

[69] A. K. Zvezdin and A. F. Popkov, Zh. Eksp. Teor. Fiz. **84**, 606 (1983) [Sov. Phys. JETP **57**, 350 (1983)].

[70] M. A. Tsankov, M. Chen, and C. E. Patton, J. Appl. Phys. **79**, 1595 (1996).

[71] B. A. Kalinikos, N. G. Kovshikov, and A. N. Slavin, Phys. Rev. B **42**, 8658 (1990).

[72] A. N. Slavin and I. V. Rojdestvenski, J. Appl. Phys. **73**, 7007 (1993).

[73] A. N. Slavin and I. V. Rojdestvenski, IEEE Trans. Magn. **30**, 37 (1994).

[74] V. L. Safonov, J. Appl. Phys. **95**, 7145 (2004).

[75] A. N. Slavin and V. Tiberkevich, IEEE Trans. Magn. **44**, 1916 (2008).

[76] T. Kasuya and R. C. Le Craw, Phys. Rev. Lett. **6**, 223 (1961).

[77] M. Sparks, *Ferromagnetic Relaxation Theory* (McGraw-Hill, New York, 1964).

[78] C. E. Patton and W. Jantz, IEEE Trans. Magn. **14**, 698 (1978).

[79] D. J. Seagle, S. H. Charap, and J. O. Artman, J. Appl. Phys. **57**, 3706 (1985).

[80] M. Chen, C. E. Patton, G. Srinivasan, and Y. T. Zhang, IEEE Trans. Magn. **25**, 3485 (1989).

[81] K. J. Harte, J. Appl. Phys. **39**, 1503 (1968).

[82] K. Yu. Guslienko and A. N. Slavin, J. Appl. Phys. **87**, 6337 (2000).

[83] R. Zivieri and R. L. Stamps, Phys. Rev. B **73**, 144422 (2006).

[84] B. A. Kalinikos and A. N. Slavin, J. Phys. C **19**, 7013 (1986).

[85] M. J. Hurben and C. E. Patton, J. Magn. Magn. Mater. **139**, 263 (1995).

[86] C. E. Zaspel, P. Kabos, H. Xia, H. Y. Zhang, and C. E. Patton, J. Appl. Phys. **85**, 8307 (1999).